AIAA JOURNAL
Vol. 49, No. 1, January 2011

Measurement and Modeling of Effect of Forward Flight on Jet Noise

K. Viswanathan* and M. J. Czech†
The Boeing Company, Seattle, Washington 98124-2207

DOI: 10.2514/1.J050719

An experimental program is carried out to assess the effects of forward flight on both turbulent mixing noise and broadband shock-associated noise from single-stream jets. Far-field spectral measurements are made over a wide range of jet operating conditions and at seven tunnel Mach numbers, in an open freejet anechoic facility. The tunnel Mach number M_t spans a range from 0.0 to 0.32. The values of the flight velocity exponent k, obtained from a least-squares fit of the variation of the reduction in overall sound pressure levels with relative velocity ($10\,\mathrm{Log}[V_j/(V_j - V_t)]$), have been calculated at all angles from the database. The flight velocity exponent has no discernible dependence on jet Mach number or temperature ratio. There is a distinct variation with angle: a slow increase from ~2.9 to ~3.5 at the lower polar angles from 50 to ~105° and a steeper increase from ~3.5 to ~7.6 from ~105 to 150°. Two different characteristic velocities may be identified for jets in forward flight: jet velocity V_j and relative velocity $(V_j - V_t)$. Though the Strouhal numbers based on both provide good collapse of the spectra at the lower polar angles, the jet velocity V_j rather than $(V_j - V_t)$ is shown to be the correct characteristic velocity at large aft angles. Thus, it is established that the regular Strouhal number based on V_j is the correct nondimensional frequency for scaling spectra. The scaling of spectra at large aft angles is not straightforward and additional issues need to be considered. For jets in the presence of forward flight, it is established that the phenomenon of nonlinear propagation is observed when the relative velocity $(V_j - V_t)$ becomes convectively supersonic. This is a new result and has not been reported in any prior study. An effective jet velocity, which is a combination of both the jet velocity and the ambient speed of sound, is required to collapse spectra from unheated jets only at large aft angles. The use of an effective velocity is not required for heated jets; the regular Strouhal number is the correct nondimensional frequency at all angles, with or without forward flight. The effect of forward flight on broadband shock-associated spectra is minor. The effects of flight on spectra at various angles need to be modeled for the development of a practical prediction scheme for jet noise. A simple additional term to the recent scaling method is shown to collapse the spectra obtained in the presence of forward flight. It is quite remarkable that the characteristics of the mixing noise spectra from single-stream jets at all angles, with or without the presence of forward flight, can be represented by a single equation. The negligible dependence of the flight velocity exponent on jet conditions allows for the following practical benefit: it is possible to predict the flight effect for lower-velocity jets for which the measurement of flight effect may not be feasible because of high tunnel-noise floor. This key finding perhaps represents the greatest value of this investigation.

Nomenclature

A	=	nozzle exit area
a	=	speed of sound in ambient medium
AA	=	atmospheric attenuation, dB/ft
D	=	nozzle diameter
F	=	spectrum function; depends on angle, Strouhal number and temperature ratio
f	=	frequency, Hz
k	=	flight velocity exponent
M	=	jet Mach number
M_t	=	tunnel or flight Mach number
n	=	velocity exponent for turbulent mixing noise
r	=	radial distance
St	=	Strouhal number, fD/V_j
St_m	=	modified Strouhal number, $fD/(V_j - V_t)$
T_a	=	ambient temperature
T_j	=	jet static temperature
T_t	=	jet stagnation temperature
V_j	=	jet velocity
V_t	=	tunnel or flight velocity
α	=	coefficient in definition of effective velocity
θ	=	inlet angle

Subscripts

a	=	ambient conditions
j	=	jet conditions

Presented as Paper 2010-3921 at the 16th AIAA/CEAS Aeroacoustics Conference, Stockholm, Sweden, 7–9 June 2010; received 13 June 2010; revision received 16 August 2010; accepted for publication 21 August 2010.

*Boeing Technical Fellow, M/S 0R-JF, P.O. Box 3707; k.viswanathan@boeing.com. Associate Fellow AIAA.

†Aeroacoustics Engineer, M/S 0R-JF, P.O. Box 3707; michael.j.czech@boeing.com. Member AIAA.

I. Introduction

IT IS well established that a jet in forward flight radiates lower levels of noise than a jet operated statically. The quantification of the effects of forward flight has received attention since the early 1970s because of its importance in the certification of aircraft for flyover noise and also for the development of prediction methods. However, the effects of forward flight on aircraft noise are difficult to quantify for a variety of reasons. Even the measurement of this effect poses a significant challenge; predictions of the flight effect are consequently harder. Flight testing of aircraft is very expensive and time-consuming. Several factors such as multiple engine noise sources, multiple engine configurations, engine installation effects and nonuniform flow around the engines, atmospheric propagation effects, varying weather conditions over very long propagation distances, ground reflection, and ground absorption at shallow grazing angles render even the interpretation of the measured data very difficult. Given this level of complexity, it is not surprising that there is no consensus on what constitutes a flight effect for individual engine noise components. In 30 years of research, many theories and the presence of additional jet noise sources due to interaction effects have been proposed to explain the observed trends. Since the early seventies, many experimental techniques have been developed that

attempt to simulate a real aircraft flyover. These have consisted of embedding the jet in a wind tunnel, jet mounted on tracked vehicles on land, jet mounted on whirling rotor arms, and taxiing aircraft. Crighton et al. [1] provided a critical evaluation of the different techniques and the advantages and disadvantages associated with each. Apart from the practical considerations of carrying out a proper test, they highlighted some fundamental issues regarding the necessity of preserving the dimensionless parameters at the model-scale and the importance of the detailed nature of the noise source and its acoustic environment, in evaluating the direct effect of flight on source strength. Many of these issues are yet to be resolved completely and are still pertinent.

Flight effects nowadays are usually assessed by embedding a jet simulator in a freejet wind tunnel of much larger diameter, in a large anechoic chamber. Von Glahn et al. [2], Cocking and Bryce [3], Bushell [4], Packman et al. [5], Plumblee [6], Tanna and Morris [7] and Cocking [8] carried out some of the earlier studies. In the wind tunnel tests, the microphones are located either in the tunnel flow or in the static environment outside the tunnel flow. The latter case of out-of-flow measurements are the easiest to carry out and one could ensure that the acoustic measurements are made in the true far field. However, corrections are needed for the propagation of sound through the tunnel shear layer. Some of the factors that need to be considered while developing these corrections are: finite thickness of the tunnel shear layer, axial spreading of the tunnel shear layer in the downstream direction, multiple reflection of sound waves between the jet and tunnel shear layers, scattering of sound by turbulence in the tunnel shear layer, background noise of the tunnel shear layer, near field interaction of the jet and tunnel shear layers if the wind tunnel is not large enough, and a few other issues such as the possible excitation of the tunnel flow by the jet and the impact of the exhaust collector. The other major issue concerns the distributed nature of the jet sources. If there is rapid variation of the correction factor with angle, it is necessary to place the microphones at a large distance from the tunnel shear layer so as to invoke the assumption of a point source. The challenging requirements of a very large wind tunnel to prevent the interaction of the two shear layers and a large anechoic chamber to ensure far-field observer location pose a tremendous problem and these requirements are not met by many facilities.

The in-flow measurements avoid this problem with the tunnel shear layer. However, the anechoicity of the tunnel is not always perfect. The problem of tunnel flow over the microphones is also an issue. The biggest concern, however, is the requirement of a very large tunnel to ensure that the microphones are in the far field, especially for a large source region.

In recent years, the out-of-flow measurements have been favored. Many of the issues with this type of arrangement mentioned above have been investigated. Amiet [9] developed analytical expressions for calculating the refraction from the shear layer assuming that the tunnel shear layer could be represented by a vortex sheet. Morfey and Tester [10] examined the various issues and recommended some guidelines on the proper choice of tunnel size, jet and tunnel operating conditions, etc., to assure good quality of data. The scattering of sound by the turbulence of the tunnel shear layer was shown to be negligible. A comprehensive study at Lockheed was carried out by Ahuja et al. [11] (see also [6]); in this study both in-flow and out-of-flow measurements at equivalent radiation angles were carried out in order to establish the corrections due to the presence of the tunnel shear layer. The proposed correction procedure was used by Tanna and Morris [7] to interpret their data. Amiet [12] evaluated the various correction procedures and the validity of the assumptions made in their derivations. All these methodologies attempt to convert the measured wind tunnel data to equivalent flyover conditions. Based on these ideas, the aircraft and engine companies have developed procedures to extrapolate the wind-on model-scale data to full-scale flyover conditions. One of the biggest differences in these methods is the prescription of the source location for a given frequency. Empirical relations for source distributions have been derived based on theoretical considerations, acoustic mirror measurements, microphones located at multiple sideline arrays, and a combination of in-flow and out-of-flow microphones. In the multiple sideline array technique, data from each array is extrapolated to a common (larger) distance, with an assumed source distribution. The multiple microphone array technique is used for the estimation of source location for static jets, but has never been used for flight corrections. Through proper modification of the source locations, the difference between the two sets of extrapolated data is driven to acceptable tolerance. However, when a novel suppressor nozzle is tested, this process has to be repeated since the source distributions could be vastly different. Not unexpectedly, the same data processed by different procedures yield slightly different noise estimates. This is not to say that there are fundamental problems with these methods; rather, the complexities are addressed and treated in different ways.

Given the variability in the interpretation of wind tunnel data, other techniques have also been attempted; a notable one is the French Bertin Aérotrain. The test nozzle is mounted on this air-cushioned tracked vehicle and acoustic testing is carried out in an open field. Hoch and Berthelot [13] provide a description of the vehicle, the model hardware, test and analysis procedure, and calibration test results. As pointed out by them, this is a flexible system offering a variety of advantages. These include independent control of the vehicle and jet operating conditions, similar acoustic environment for static and in-flight conditions, and the ability to reproduce an actual flyover event at greatly reduced cost. There are some problems such as the self-noise of the vehicle and the ground effect, which need to be considered in this type of measurement. Hoch and Berthelot [13] report the many steps taken to minimize the parasitic and nonjet noise and demonstrate good data quality for nozzle pressure ratios greater than $\sim$1.6. Drevet et al. [14], in a companion paper, provide detailed test results of flight effects on both turbulent mixing noise and broadband shock-associated noise.

Norum and Shearin [15] made measurements of the far-field acoustic characteristics and the plume fields of unheated supersonic jets in an open wind tunnel in the tunnel Mach number range of 0.0–0.4. Norum and Brown [16] extended the range of tunnel Mach number by using a freejet of one-foot diameter, and carried out aerodynamic and acoustic measurements from small convergent and C-D nozzles ($D = 0.75$ in.) operated isothermally. The Mach number of the freejet could be as high as 0.9. They noticed that the plume characteristics could be altered significantly when the freejet Mach number was increased to higher values. However, there were negligible changes to the broadband shock noise for tunnel Mach numbers up to $\sim$0.6.

Though these studies gathered much information, there are significant gaps in the data; for example, the frequency range was limited in the earlier tests. Further, good spectral measurements over a wide range of angles are not readily available. To address this deficiency, an aeroacoustic test program has been completed. A comprehensive database has been created for heated and unheated single-stream and dual-stream jets at several flight Mach numbers. The salient results for single-stream jets are reported in this paper. Section II provides details of the experimental program; a description of the processing of the data is provided in Sec. III. The main results are presented and discussed in Sec. IV. Finally, a summary of the main findings is reported in Sec. V.

II. Experimental Program

The aeroacoustic test has been carried out at Boeing's Low Speed Aeroacoustic Facility. Detailed descriptions of the test facility, the jet simulator, the data acquisition and reduction process, etc., may be found in [17–19]. For the sake of completeness, a brief overview is provided here. Bruel and Kjaer quarter-inch Type 4939 microphones are used for free-field measurements. The microphones are set at normal incidence and without the protective grid, which yields a flat frequency response up to 100 kHz. Typically, several microphone arrays are used; these arrays are at a constant sideline distance of 15 ft (4.572 m) from the jet axis and on a polar arc of 25 ft (7.62 m). All angles are measured from the jet inlet axis, and cover a polar range of 50 to 150°. Very fine narrow band data with a bin spacing of 23.4 Hz up to a maximum frequency of 88, 320 Hz are acquired and synthesized to produce one-third octave spectra, with a center band

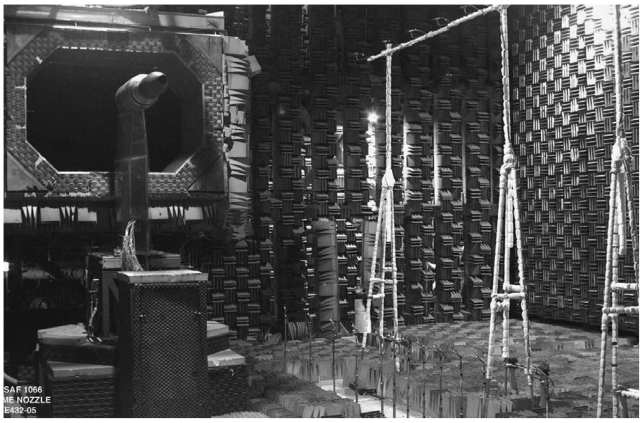

Fig. 1 Photograph of low-speed aeroacoustic facility showing the anechoic chamber, the jet rig, the freejet wind tunnel and some of the microphones.

frequency range of 200 to 80,000 Hz. The jet simulator is embedded in a freejet wind tunnel, which can reach a maximum Mach number of 0.32. The dimension of the wind tunnel is 9 by 7 ft. Figure 1 shows a photograph of the jet simulator, the wind tunnel and several microphones. The nozzle diameter is 2.45 in. (6.2 cm) and has an aerodynamic external fairing that enables proper operation with the freestream flow. In addition, there is a suction system for controlling the boundary layer. External boundary layer measurements have been made on the jet simulator. The features of the suction system and the characteristics of the boundary layer were reported in Viswanathan [17]; see Sec. III.C.2 in that paper. These issues are not repeated in the current article. Jets at several subsonic and supersonic Mach numbers (M) and stagnation temperature ratios (T_t/T_a) have been included in the test matrix. Acoustic data at seven freestream Mach numbers (M_t) of 0.0, 0.12, 0.16, 0.20, 0.24, 0.28 and 0.32 have been obtained. The acoustic rays from the jet are subject to two effects: 1) convection in the downstream direction due to the freestream and 2) refraction due to the tunnel shear layer. The changes in the spectral amplitude and the radiation angle due to the coflow have been calculated using the procedure developed by Amiet [9,12]. An interpolation of the resulting spectra at the true radiation angles to the radiation angles for the static case (fixed microphone angles) allows the direct comparison of the spectra obtained at various tunnel Mach numbers. The changes in spectra due to the effect of forward flight are assessed at various jet and tunnel conditions.

III. Processing of the Data

The as-measured data are corrected to a common distance of 20 ft (6.096 m) from the center of the nozzle exit (coordinate system with origin at the center of the nozzle exit) and lossless conditions. The atmospheric attenuation coefficients are obtained from the method of Shields and Bass [20]. Implicit in this process is the assumption of linear propagation, with the sound pressure level (SPL) obeying the $(1/r^2)$ dependence. The normalization process may be written as

$$\mathrm{SPL}_{(20\ \mathrm{ft})} = \mathrm{SPL}_{\mathrm{measured}} - 10\ \mathrm{Log}_{10}\left(\frac{20}{r}\right)^2 + r[AA_{(\mathrm{test\ day})}]$$

where r (ft) is the distance of the microphone from the origin of the coordinate system, AA are the atmospheric absorption coefficients (which are frequency dependent) per foot. The above equation provides spectra corrected to lossless conditions; lossless spectra are presented throughout this paper. The accuracy of the weather corrections and the suitability of the different proposed methods have been evaluated by Viswanathan [21]; it was shown that the method of Shields and Bass [20] was the best at the higher frequencies of interest in model-scale tests. For the jet with a coflow, the propagation distance to the microphone needs to account for the convection and refraction effects; again, the method of Amiet [9,12] together with the geometry of the jet and the wind tunnel are used to calculate the actual distance traveled by the acoustic rays. The distributed sources of the jet are assumed to be represented by a point source located at the center of the nozzle exit plane. It has been shown in [22,23] that the microphones are indeed located in the true acoustic and geometric far field for the nozzle diameter used here. In the current paper, the spectra obtained with the microphones on the 25 ft polar array are used. The nondimensional distance (r/D) to the microphones is 122. Viswanathan [23], in order to determine the minimum distance to the far field, investigated 1) the source distributions and 2) the directivity characteristics of unheated and heated jets with a Mach number range of 0.5–1.92 with a variety of measurements, together with the polar response characteristics of condenser microphones. The geometric and acoustic far field is defined as the distance at (and beyond) which the distributed sources in a jet can be represented by a point source located on the jet axis at

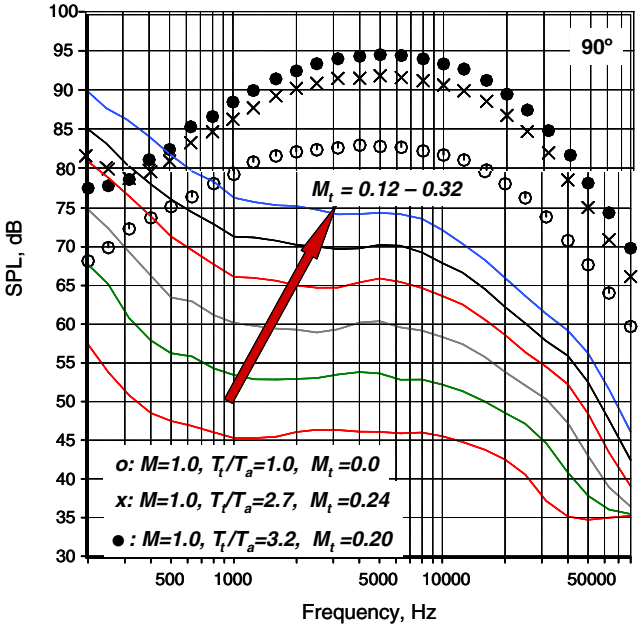

a)

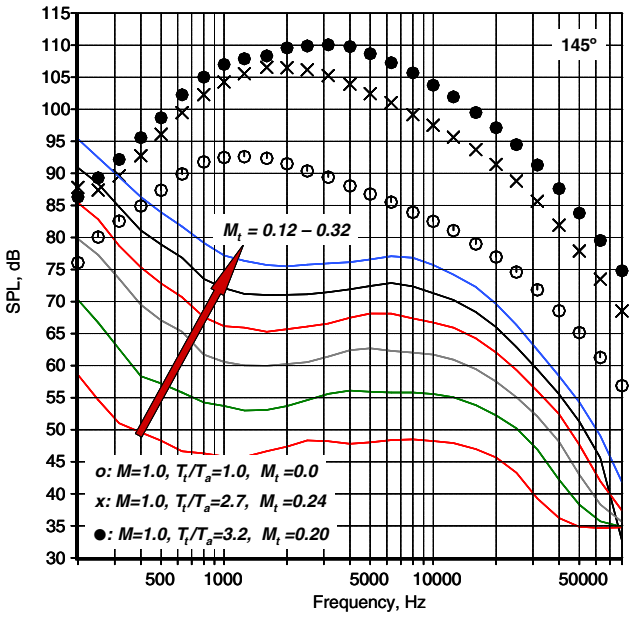

b)

Fig. 2 As-measured one-third octave spectra: tunnel noise floors and from jets at different operating conditions.

the nozzle exit plane. It was shown unambiguously that for all frequencies from 200 Hz–80 kHz,

1) A nondimensional distance of 40D represents the true far field for subsonic jets at all temperature ratios.

2) 40D again represents the true far field for unheated supersonic jets.

3) A distance of $\sim$70D is prudent for highly heated supersonic jets, especially in the angular range of $\sim$110 to $\sim$125°. Given the much larger distance to the microphones (122D) in the current dataset, the assumption of a point source at the nozzle exit plane in the processing of the data is justified. For the wind-on case, the proper values of the atmospheric attenuations inside and outside the tunnel flow are used. Narrowband spectra are shown only when supersonic jets are considered; the rich spectral details, especially for shock-associated noise, tend to get washed out in the integration for one-third octave spectra. It is noted that only one-third octave spectra are shown for all subsonic cases.

IV. Results and Discussion

A. Quantification of Flight Effect and Impact of Tunnel Noise

It is important to understand at the outset the noise generated by the jet and the wind tunnel so that meaningful measurements, uncontaminated by the tunnel noise floor, are made. Sample as-measured one-third octave spectra at two inlet angles of 90 and 145°, together with the tunnel noise floor are shown in Fig. 2. The tunnel noise at 6 Mach numbers of 0.12, 0.16, 0.20, 0.24, 0.28 and 0.32, denoted by lines, show the expected monotonic increase with M_t. Given the large size of the tunnel, the peak levels occur at 200 Hz. Three as-measured spectra are also included; the jet conditions are 1) $M = 1.0$, $T_t/T_a = 1.0$, and $M_t = 0.0$; 2) $M = 1.0$, $T_t/T_a = 2.7$, and $M_t = 0.24$; and 3) $M = 1.0$, $T_t/T_a = 3.2$, and $M_t = 0.20$. It is clear that the low-frequency portions of the jet spectra can be impacted by the high levels of the wind tunnel noise floor; it can also be deduced that it would be difficult to make wind-on measurements for unheated jets, at high tunnel velocities. At 90°, the spectrum from the jet with $M = 1.0$, $T_t/T_a = 2.7$, and $M_t = 0.24$ exhibits a tail-up at the lowest $\sim$3 frequency bands due to contamination from the tunnel noise floor (third curve from top). At lower inlet angles in the forward quadrant, this problem is exacerbated because the jet noise levels are low. In the peak radiation sector at large aft angles, the spectral levels increase considerably, especially for heated jets. Consequently, there is a larger separation between the jet noise spectra and the tunnel noise floor levels. These sample spectra highlight the various issues and the interplay between the noise floor and the jet spectral levels at different radiation angles.

Spectral comparisons that quantify the effect of forward flight are now presented. Lossless processed data are shown; the raw frequencies are used on the x-axis for the time being. The proper nondimensional frequency for scaling the spectra is determined in

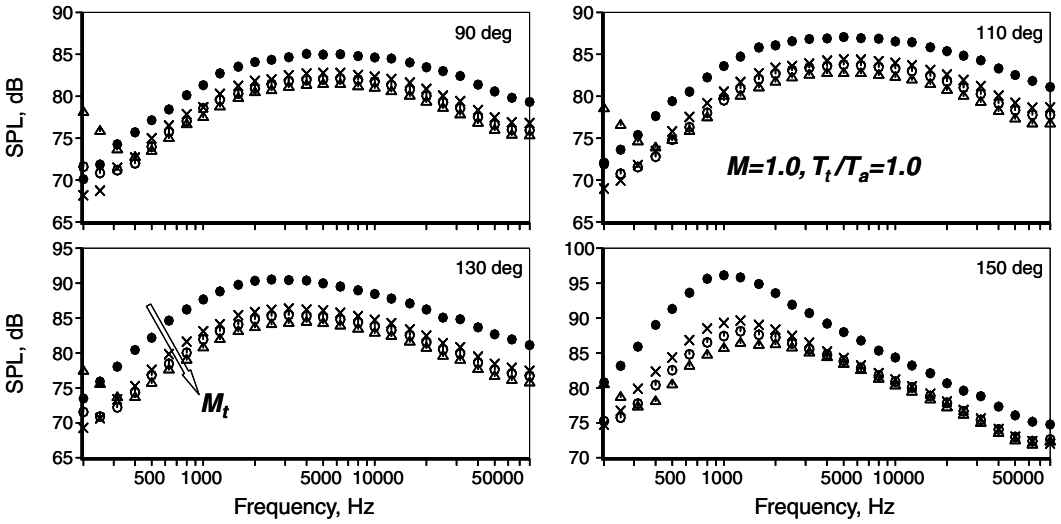

Fig. 3 Effect of forward flight on spectra. $M = 1.0$, $T_t/T_a = 1.0$. ●: $Mt = 0.0$; ×: 0.12; ○: 0.16; △: 0.20.

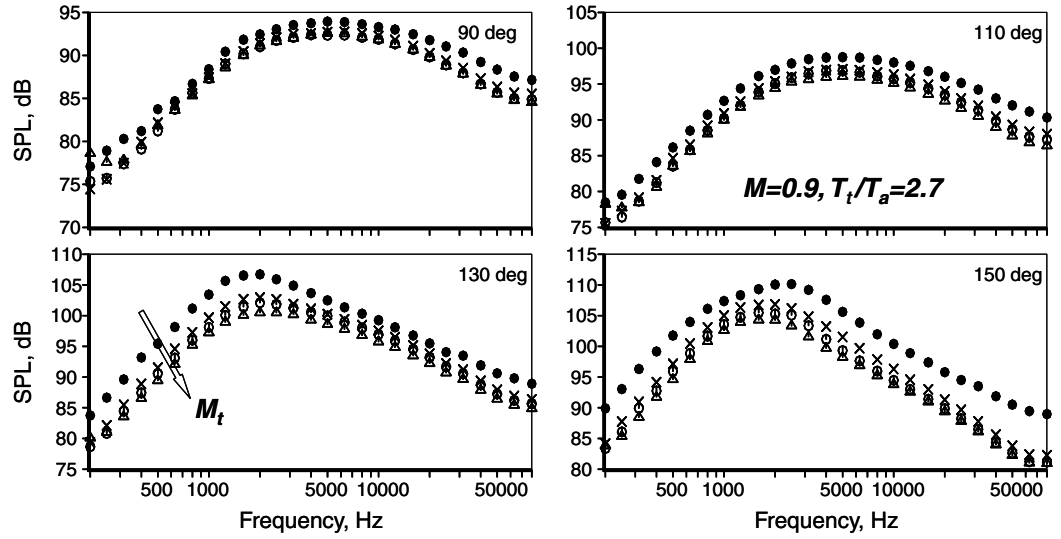

Fig. 4 Effect of forward flight on spectra. $M = 0.9$, $T_t/T_a = 2.7$. ●: $Mt = 0.0$; ×: 0.12; ○: 0.16; △: 0.20.

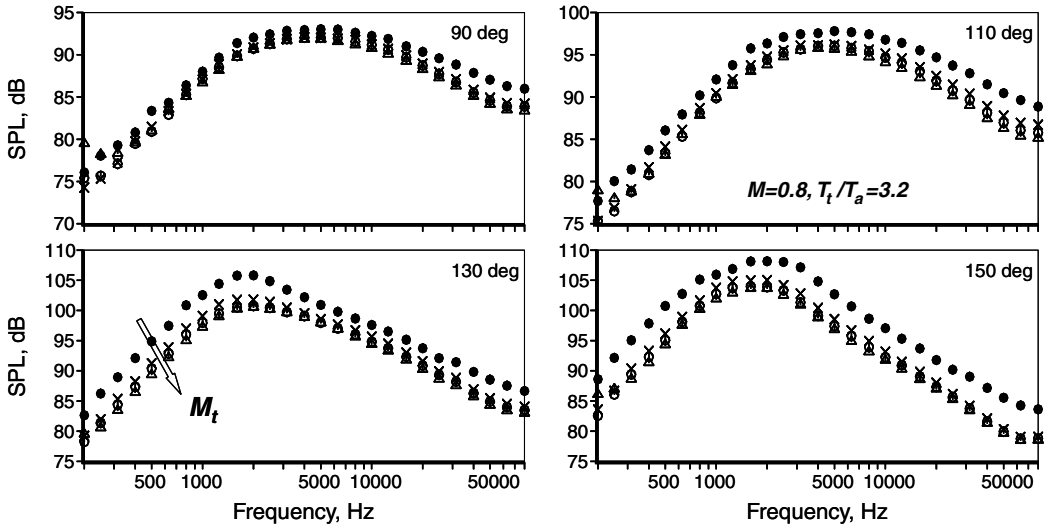

Fig. 5 Effect of forward flight on spectra. $M = 0.8$, $T_t/T_a = 3.2$. ●: $Mt = 0.0$; ×: 0.12; ○: 0.16; △: 0.20.

the next section. Figure 3 shows spectral comparisons at four radiation angles for an $M = 1.0$ and $T_t/T_a = 1.0$ jet at four tunnel Mach numbers of 0.0, 0.12, 0.16, and 0.20. The arrow indicates the direction of increasing M_t. The expected monotonic decrease in levels with increasing M_t is observed at all angles; furthermore, the reductions in levels are fairly uniform at all frequencies at 90° and lower radiation angles (not shown). At the very low frequencies, there is a tail-up in the spectra because of contamination from the tunnel noise floor at higher M_t, especially for the $M_t = 0.20$ case (denoted by the triangles). At large aft angles, the trends are noticeably different: a large reduction of ∼8 to ∼13 dB is observed at the spectral peak at 150°; the reduction is ∼5 dB at the higher frequencies.

Figures 4 and 5 depict the effects of forward flight for heated jets, with tunnel Mach numbers of 0.0, 0.12, 0.16 and 0.20. The jet operating conditions are $M = 0.9$, $T_t/T_a = 2.7$, and $M = 0.8$, $T_t/T_a = 3.2$, respectively. There are some clear differences between the effects of forward flight for heated and cold jets: the absolute magnitude of noise reduction for a given tunnel Mach number is lower for heated jets. The strong reduction near the spectral peak, observed for the cold jet at large aft angles, is absent for the heated jets and the spectral reduction is more uniform over the entire frequency range. Similar trends are observed for other heated jets; these results are not included but will be presented as part of the following sections.

B. Scaling of Spectra with Forward Flight

Most of the past studies on scaling of the effect of forward flight have mainly concentrated on the overall sound pressure levels (OASPL) at various radiation angles; see for example Tanna and Morris [7] and Michalke and Michel [24]. In the experiments at Lockheed, an exponent of 5 to 5.5 based on the relative velocity has been found to predict the reduction in OASPL, especially at 90°. However, there is considerable scatter in the calculated exponent for relative velocity, as noted in Fig. 1.1 in [11]. The effects of flight on spectra at various angles need to be modeled for the development of a practical prediction scheme for jet noise. The recent scaling method of Viswanathan [19,25] provides excellent collapse of the spectra at all angles and over the entire frequency range without any theoretical assumptions, thereby permitting the development of an accurate prediction method for jets in a static environment. The spectrum at every angle is described by the product of a shape function dependent on the jet temperature ratio and the velocity ratio raised to a velocity exponent, which is a function of angle and temperature ratio. One of the goals of the present study is the extension of the basic methodology to include flight effects. This topic is addressed in Sec. IV.E.

A relative velocity exponent, based on the measured OASPL, can be calculated from the measured data at each angle. The measured reduction in OASPL is plotted against the parameter $[10* \mathrm{Log10}(V_j/(V_j - V_t))]$; here, V_j is the jet velocity and V_t is the tunnel velocity. Least-squares fit through the data yields the value of the exponent. The entire database has been processed and the values of the relative velocity exponent (k) at all angles have been determined. A cautious approach vis-à-vis contamination by tunnel noise at the lower frequency regime has been adopted; this issue is critical especially 1) at the lower radiation angles where jet noise levels are low and 2) for lower velocity jets at the higher tunnel Mach numbers.

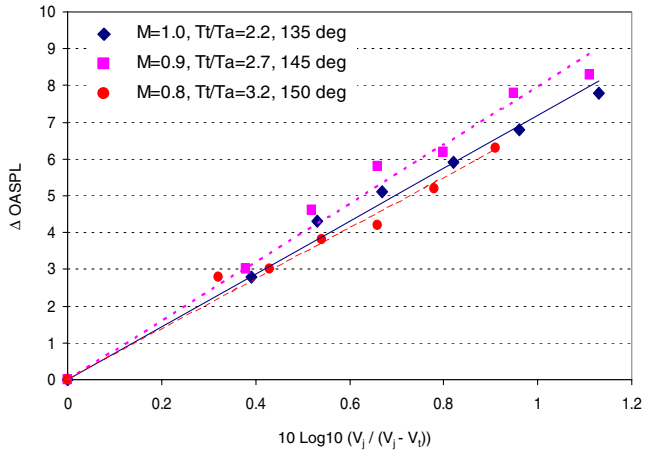

Fig. 6 Curve-fits for the relative velocity exponent at large aft angles.

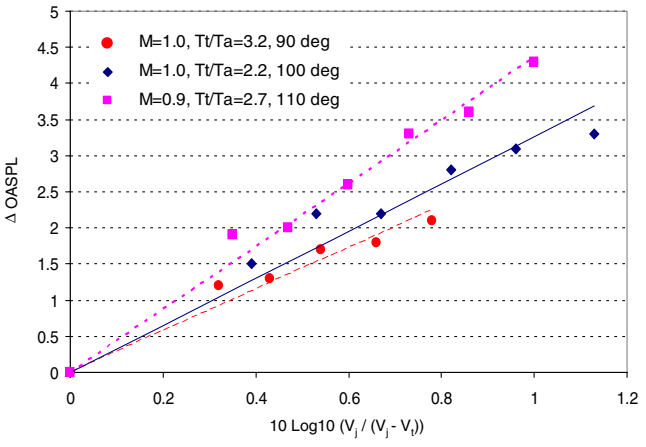

Fig. 7 Curve-fits for the relative velocity exponent at lower inlet angles.

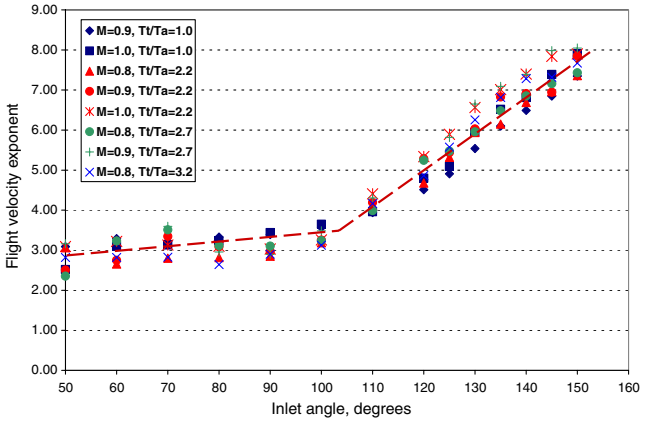

Fig. 8 Variation of the relative velocity exponent with radiation angle; various jet conditions.

In practice, the measured spectra together with the tunnel noise floors have been examined at every angle and every jet condition. Whenever the tunnel noise floor led to an upturn in spectra at the lower frequencies, the spectra at that tunnel Mach number was not included in the computation of the relative velocity exponent. For example, spectra at only the lowest four tunnel Mach numbers might be included at 60° for an unheated jet with $M = 0.9$, whereas the data obtained at six or seven tunnel Mach numbers might be included at aft angles for a jet with $M = 0.9$ and $T_t/T_a = 3.2$. Thus, data contaminated by tunnel noise are simply ignored.

Sample curve-fits are shown in Figs. 6 and 7, respectively. Three different aft angles and three different jet conditions are chosen in Fig. 6. Least square fits through the measured values are also plotted in the figure. Good linear variations are exhibited by the measured data points. The values of the exponents are 7.41, 7.98, and 7.32 at 135°, 145° and 150°, respectively. It should be pointed out that the values for the exponent can change slightly, by ∼0.25, depending on the data points included in the curve-fits. Similar linear trends are observed at three lower radiation angles in Fig. 7. The variations of the velocity exponents with radiation angle for eight jet conditions are shown in Fig. 8. The first striking observation is the following: the values of the relative velocity exponent at different jet conditions do not have a strong dependence on jet Mach number or temperature ratio, and are tightly clustered at each angle. The dashed red line denotes a mean trend line through the values. Secondly, there is a distinct variation with angle: a slow increase from ∼2.9 to ∼3.5 at the lower polar angles from 50 to ∼105° and a steeper increase from ∼3.5 to ∼7.6 from ∼105 to 150°. There is remarkable similarity between the directivity curves for the relative velocity exponent and the velocity exponent for turbulent mixing noise (see Fig. 16 in Viswanathan [19]): slow variation at the lower polar angles and a steep increase in the aft quadrant.

Now we demonstrate that the spectra at various tunnel Mach numbers can be collapsed with the calculated relative velocity exponents. Recall that the raw frequency is used on the x-axis for the spectral plots shown in Figs. 3–5. There are two choices for the nondimensional frequency: the regular Strouhal number based on jet velocity and a modified Strouhal number based on the relative velocity. These two may be written as

$$St = \frac{fD}{V_j} \qquad St_m = \frac{fD}{(V_j - V_t)}$$

D is the jet diameter and f is the frequency in Hertz. The suitability of both of these is examined below. Figure 9 shows normalized one-third octave spectra at 90° plotted against the regular Strouhal number. The jet conditions are $M = 1.0$ and $T_t/T_a = 1.0$ in Fig. 9a, and $M = 1.0$ and $T_t/T_a = 3.2$ in Fig. 9b. The quantity $[\mathrm{SPL} + 10 * k * \mathrm{Log10}(V_j/(V_j - V_t))]$ is plotted on the y-axis. Note that the normalization term is added to the raw SPL because the change in noise due to the tunnel flow (which is actually a reduction) is taken to be a positive quantity in the computation of the relative velocity exponent. An examination of the ordinates and the increasing values of ΔOASPL with increasing tunnel velocity observed in Figs. 6 and 7 dictate that the normalization term should be added to the measured SPL. There is very good collapse of the spectra obtained at various values of M_t of 0.0, 0.12, 0.16, 0.20 and 0.24. Note that the normalized spectra in Fig. 9a are obtained from the raw spectra at 90° shown in Fig. 3. The contamination due to the tunnel noise floor is also evident at the lowest frequencies; the magnitude of contamination is more pronounced for the unheated jet, given the lower levels of jet noise. The same data for the heated jet are plotted against the modified Strouhal number in Fig. 10. Again, there is equally good collapse when the spectra are plotted against the modified Strouhal number. An examination of the normalized spectra at other lower angles in the forward quadrant (not shown) indicates that there is good collapse of the spectra with both Strouhal

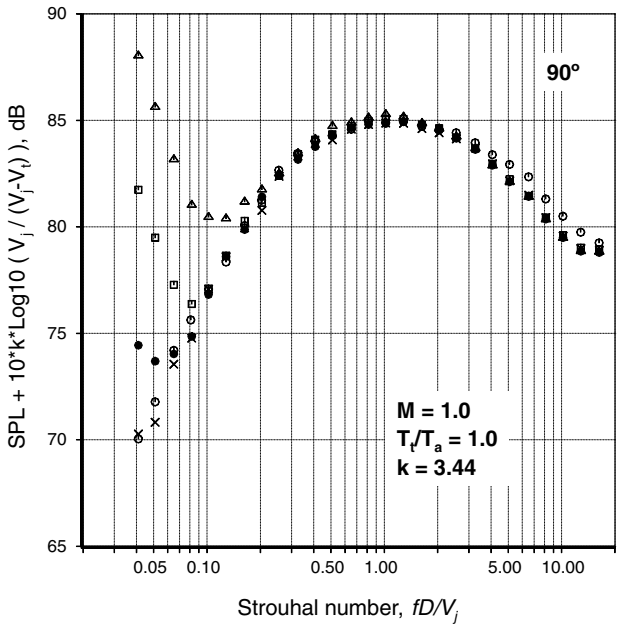

a)

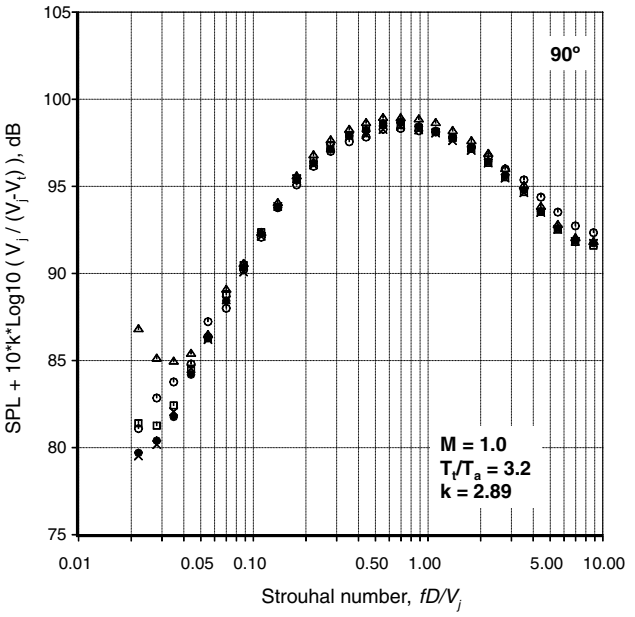

b)

Fig. 9 Normalized one-third octave spectra at 90°: a) $M = 1.0$, $T_t/T_a = 1.0$; and b) $M = 1.0$, $T_t/T_a = 3.2$. ○: $M_t = 0.0$; ×: $M_t = 0.12$; ●: $M_t = 0.16$; □: $M_t = 0.20$; △: $M_t = 0.24$.

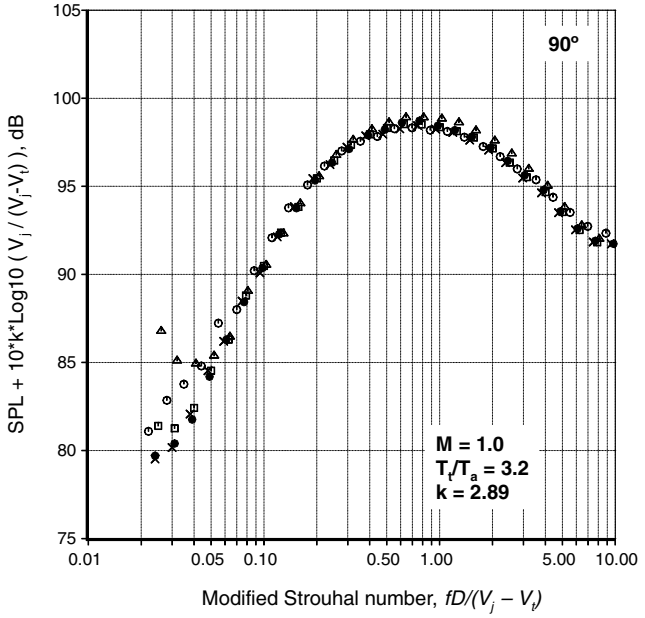

Fig. 10 Normalized one-third octave spectra at 90°. $M = 1.0$, $T_t/T_a = 3.2$. ○: $M_t = 0.0$; ×: $M_t = 0.12$; ●: $M_t = 0.16$; □: $M_t = 0.20$; △: $M_t = 0.24$.

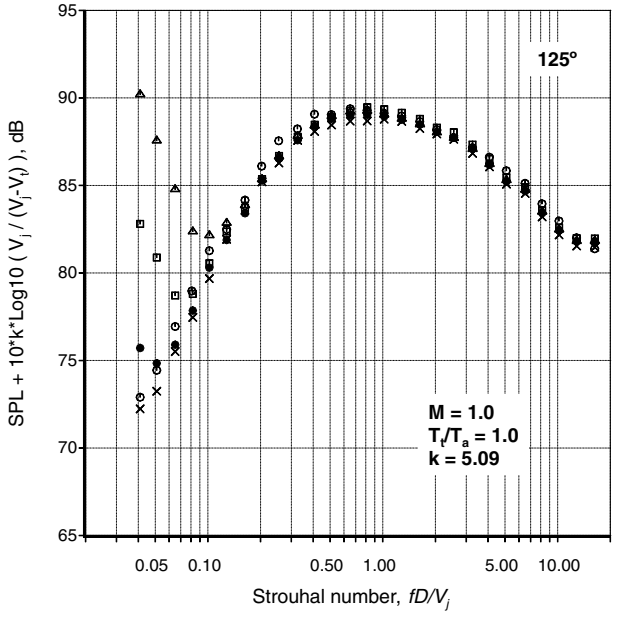

Fig. 12 Normalized one-third octave spectra at 125°. $M = 1.0$, $T_t/T_a = 1.0$. ○: $M_t = 0.0$; ×: $M_t = 0.12$; ●: $M_t = 0.16$; □: $M_t = 0.20$; △: $M_t = 0.24$.

numbers. It would appear, as of now, that both Strouhal numbers are suitable for collapsing spectra. However, this is not the case as will be made clear below.

Normalized spectra at another jet condition of $M = 1.0$ and $T_t/T_a = 2.2$ against the regular Strouhal number at 120° are shown in Fig. 11. Spectra at all seven tunnel Mach numbers of 0.0, 0.12, 0.16, 0.20, 0.24, 0.28 and 0.32 are included. The increasing level of contamination from the tunnel noise floor with increasing M_t is obvious at the lower frequencies; both the magnitude and the affected frequency range become pronounced with higher M_t. Apart from this trend, one can observe excellent collapse in the frequency range $St \geq \sim 0.09$. A sample spectral collapse for an unheated jet with $M = 1.0$ at 125° is shown in Fig. 12. Given the lower level of jet noise generated by the cold jet, the magnitude of the contamination is substantial for $M_t = 0.24$, and even for $M_t = 0.20$. Apart from this fact, there is good collapse of the spectra at the higher frequencies. Attention is drawn to another aspect of data collapse: the flight velocity exponent has been calculated only using data uncontaminated by the tunnel noise floor (at lower M_t). However, in Figs. 11 and 12, spectra at higher M_t are also shown. Given the excellent collapse at the higher frequencies not subject to contamination by tunnel noise, it is obvious that the calculated values for the flight exponents are accurate and are applicable over a wider range of tunnel Mach numbers.

Let us consider a still higher angle of 130° in Fig. 13, with jet condition of $M = 0.8$ and $T_t/T_a = 3.2$. The normalized spectra obtained with $M_t = 0.0$, 0.12, 0.16, 0.20, 0.24 and 0.28 are plotted against the Strouhal number. The degree of collapse is comparable to those seen at the lower angles. The same spectra are plotted against the modified Strouhal number in Fig. 14. There is a drastic effect now,

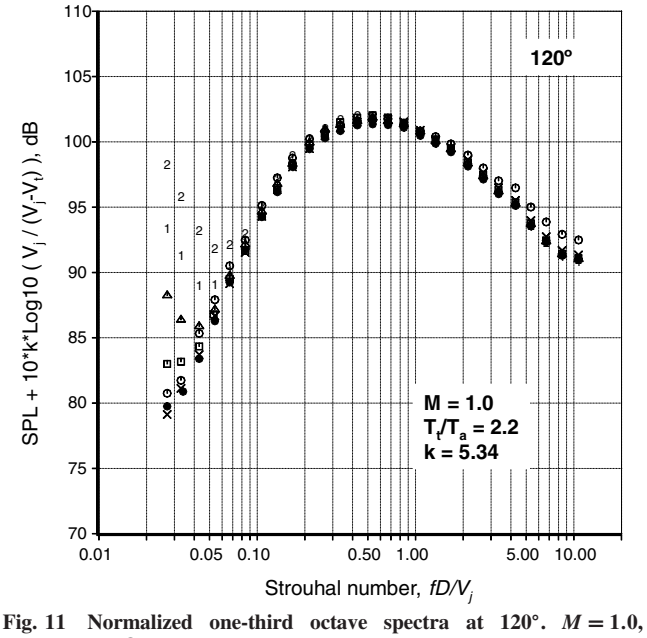

Fig. 11 Normalized one-third octave spectra at 120°. $M = 1.0$, $T_t/T_a = 2.2$. ○: $M_t = 0.0$; ×: $M_t = 0.12$; ●: $M_t = 0.16$; □: $M_t = 0.20$; △: $M_t = 0.24$; 1: $M_t = 0.28$; 2: $M_t = 0.32$.

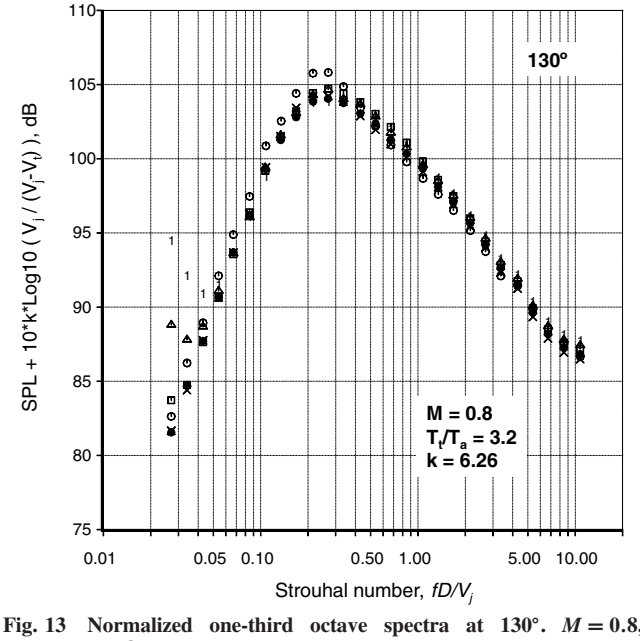

Fig. 13 Normalized one-third octave spectra at 130°. $M = 0.8$, $T_t/T_a = 3.2$. ○: $M_t = 0.0$; ×: $M_t = 0.12$; ●: $M_t = 0.16$; □: $M_t = 0.20$; △: $M_t = 0.24$; 1: $M_t = 0.28$.

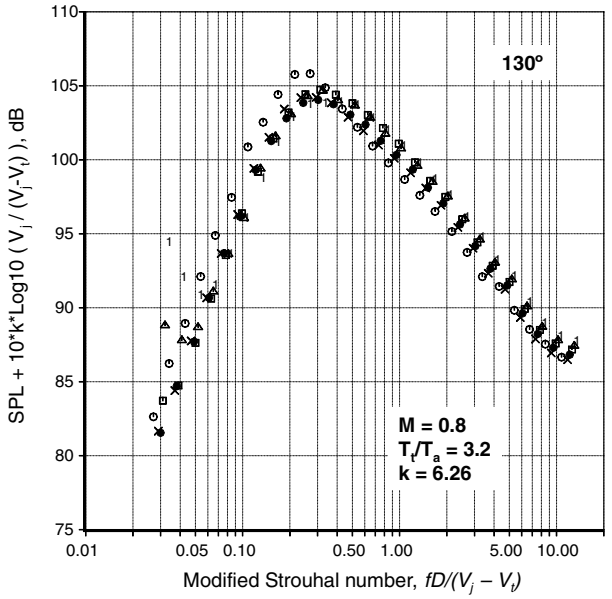

Fig. 14 Normalized one-third octave spectra at 130°. $M = 0.8$, $T_t/T_a = 3.2$. ○: $M_t = 0.0$; ×: $M_t = 0.12$; ●: $M_t = 0.16$; □: $M_t = 0.20$; △: $M_t = 0.24$; 1: $M_t = 0.28$.

and the good collapse observed in Fig. 13 is destroyed. Thus, the choice of the modified Strouhal number is detrimental to the proper scaling of spectra. A thorough examination of the use of the modified Strouhal number at other jet conditions and at other aft angles (not included here) reveals that the good spectral collapse obtained with the regular Strouhal number is vitiated when using the modified Strouhal number. As illustrated in Figs. 9–13, the regular Strouhal number is the correct nondimensional frequency for scaling spectra. This fact will be further substantiated for heated jets at higher aft angles in the following sections.

C. Additional Issues at Large Aft Angles

A few additional issues that pertain to the characteristics as well as the scaling of spectra at radiation angles $\geq \sim 125°$ are pertinent and must be considered. Viswanathan [19,25,26] has provided detailed treatments of these issues in the peak noise radiation sector for unheated and heated jets, under static conditions. The effects of forward flight are now considered.

1. *Nonlinear Propagation*

The phenomenon of nonlinear propagation in jet noise has received considerable attention in the past few years, mainly in connection with the noise of fighter aircraft. The jet velocities at typical takeoff power for these aircraft are usually $\geq \sim 2700$ ft/s (825 m/s); with the operation of afterburners, these values increase to ~ 3300 ft/s (1000 m/s). Viswanathan [21,27] offered experimental evidence that this phenomenon is observed even for subsonic heated jets at laboratory scale. Specifically, the convective Mach number was identified as a reliable parameter for predicting the onset of nonlinear propagation effects in jet noise. When the convective velocity, taken to be $0.7 * (V_j/a)$, exceeds the ambient speed of sound, nonlinear propagation effects are observed in the peak radiation sector in the aft angles. Here, a is the speed of sound in the ambient medium. In physical terms, this condition corresponds to ~ 1604 ft/s (490 m/s). When the jet velocity is increased, there is a broadening of the polar angular sector in which the main effect of transfer of energy to the higher frequencies in the jet noise spectra is manifested.

Figure 15 shows typical lossless spectra under static conditions at four aft angles of 120, 130, 140 and 150° from jets at fixed temperature ratio of 2.7 and at four Mach numbers of 0.8, 1.0, 1.37 and 1.57. The jet velocities are 1391, 1692, 2158 and 2381 ft/s, respectively. The jets are convectively supersonic for $M = 1.0$, 1.37 and 1.57. An examination of the spectra in Fig. 15 indicates the following trends:

1) At the two lower polar angles of 120 and 130°, the spectra for the subsonic jets have similar shapes, while there is a substantial increase in the spectral levels at the higher frequencies for the two supersonic

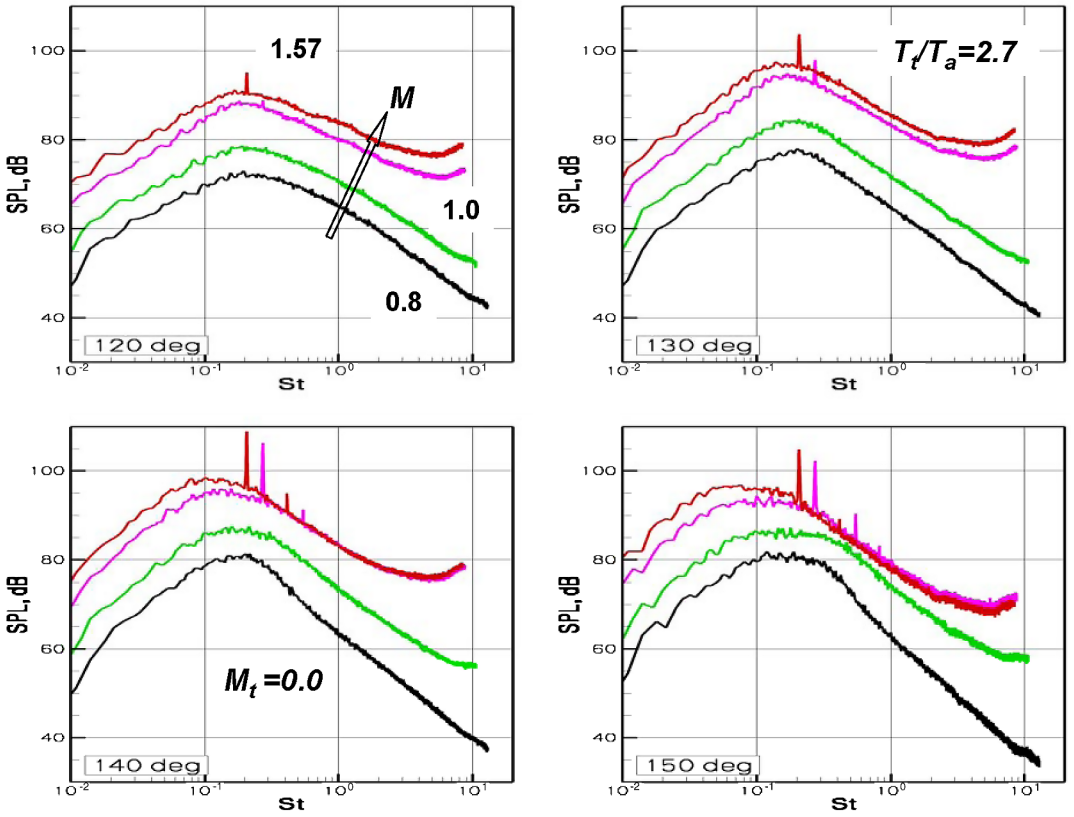

Fig. 15 Narrowband spectra at four aft angles. $T_t/T_a = 2.7$ and $M_t = 0.0$. $M = 0.8$, 1.0, 1.37 and 1.57.

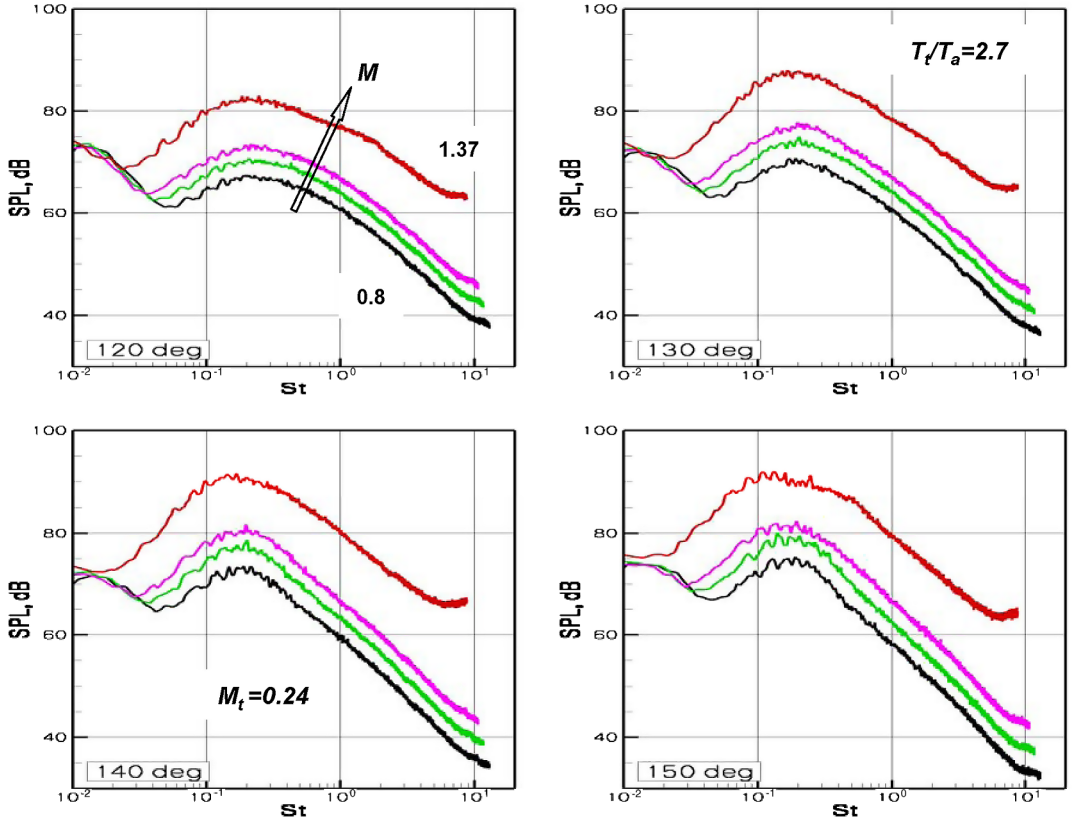

Fig. 16 Narrowband spectra at four aft angles. $T_t/T_a = 2.7$ and $M_t = 0.24$. $M = 0.8$, 0.9, 1.0, and 1.37.

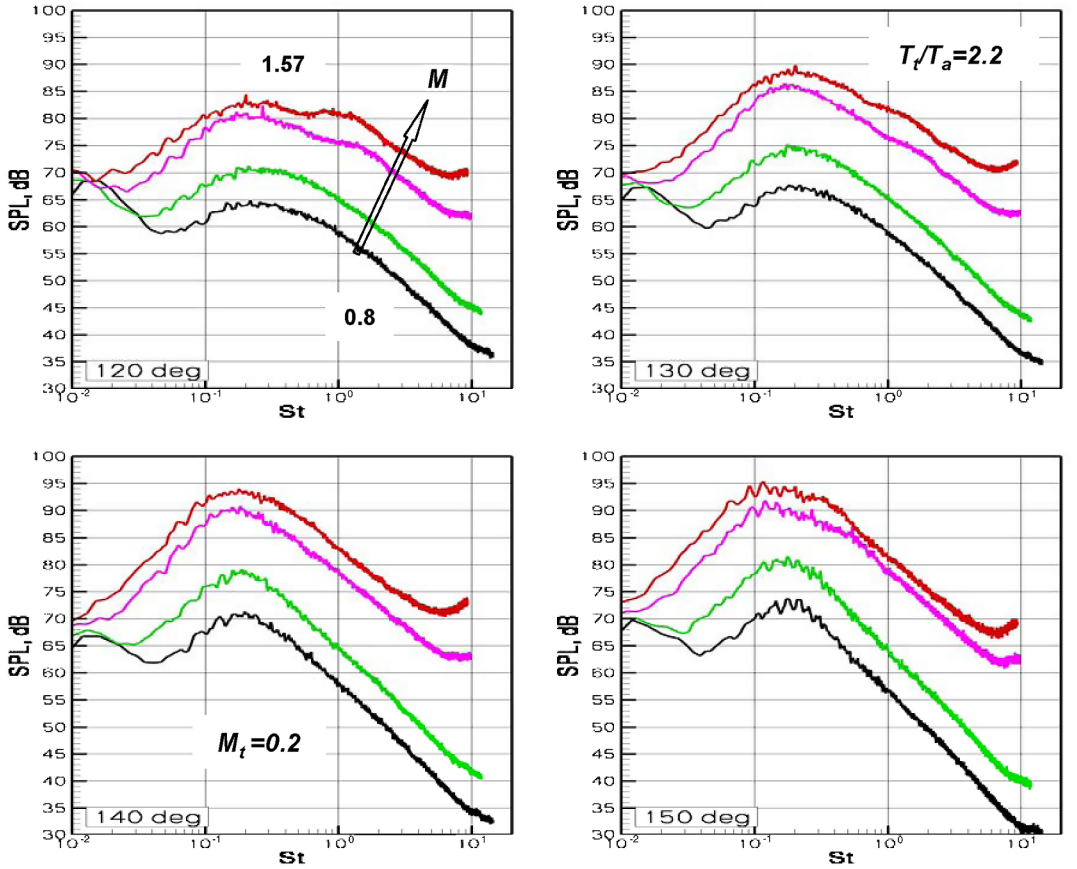

Fig. 17 Narrowband spectra at four aft angles. $T_t/T_a = 2.2$ and $M_t = 0.2$. $M = 0.8$, 1.0, 1.37 and 1.57.

jets. For instance, there is an increase in level of ~20 dB at the spectral peak ($St = \sim 0.2$) at 130° when the Mach number is increased from 0.8 to 1.57. However, at a high Strouhal number of ~10, the increase in level is almost 40 dB. The reason for the larger increase is due to the transfer of energy from the spectral peak to the higher frequencies, associated with effects of nonlinear propagation, for the convectively supersonic jet. There is a drastic change in the spectral shape at $M = 1.57$, with a curl-up at the higher frequencies, which is a manifestation of nonlinear propagation effects. In contrast, there is a monotonic decrease in level with increasing Strouhal number for the $M = 0.8$ jet.

2) At the higher angles of 140 and 150°, nonlinear trends are observed for all three jets with convectively supersonic velocities.

3) For the supersonic jets, the nonlinear effects are observed over a larger angular sector. Figure 16 shows another case at the same temperature ratio of 2.7 and four Mach numbers of 0.8, 0.9, 1.0 and 1.37; the tunnel Mach number is 0.24, with $V_t = 261$ ft/s. Now, the spectral shapes are similar for the three subsonic jets at all the radiation angles with the nonlinear effects present only for the jet

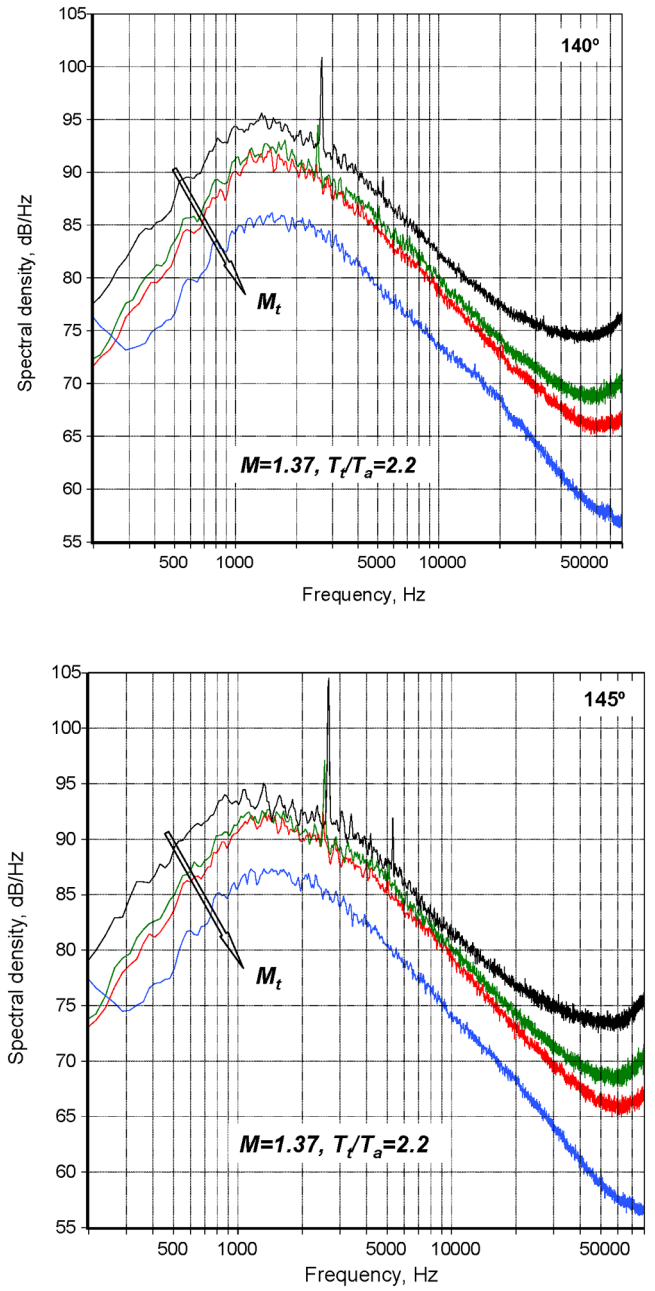

Fig. 18 Narrowband spectra at two aft angles. $M = 1.37$, $T_t/T_a = 2.2$ and $M_t = 0.0$, 0.12, 0.16 and 0.32.

with $M = 1.37$. The biggest difference between Figs. 15 and 16 is the following: nonlinear effects are suppressed for the $M = 1.0$ jet at 140 and 150°.

The spectra at the same four aft angles for a different jet condition of $T_t/T_a = 2.2$ and $M = 0.8$, 1.0, 1.37 and 1.57 are presented in Fig. 17. The tunnel Mach number is 0.20, with $V_t = 217$ ft/s. The jet velocities are 1254, 1524, 1943 and 2142 ft/s, respectively. The velocities of the subsonic jets are below the threshold value of ~1604 ft/s; consequently nonlinear effects are suppressed. Figure 18 depicts spectra at two aft angles of 140 and 145° for the following jet conditions: $M = 1.37$, $T_t/T_a = 2.2$ and $V_j = 1943$ ft/s. Now, the jet conditions are fixed and the tunnel Mach number is increased from 0.0 to 0.12, 0.16 and 0.32. The corresponding tunnel velocities are 0.0, 131, 174 and 348 ft/s, respectively. There is a dramatic difference in the spectral shapes at both angles when the tunnel velocity reaches 348 ft/s. For this tunnel condition, the relative velocity $(V_j - V_t)$ is 1595 ft/s, just below the threshold value and the nonlinear propagation effects, whereby energy is transferred to the higher frequencies and the spectrum starts curling up, suddenly ceases. This feature is again highlighted with a $M = 1.0$, $T_t/T_a = 3.2$ and $V_j = 1846$ ft/s jet in Fig. 19. The tunnel velocities are 0.0, 131 and 348 ft/s. Again, the tail-up at the highest frequencies is absent at 140 and 150° when the tunnel velocity is increased to 348 ft/s, because the relative velocity drops to 1498 ft/s. One can confirm these trends by calculating the Morfey–Howell indicators [28] from the time-series signals for these test cases. See [21,29] for more details. However, this process is quite involved for the wind-on cases: the wave-normal or true radiation angle keeps changing with the tunnel Mach number. For spectral comparisons, an interpolation routine provides the spectra at the fixed microphone angles, as already noted. A proper way to accomplish this task would entail moving the microphone to predetermined radiation angles for the wind-on cases. This complication placed unacceptable delay in the test schedule and hence is not adopted in this test. From a comprehensive analysis of the entire database, the following condition for the onset of nonlinear propagation effects in jets subjected to forward flight is identified: the relative velocity $(V_j - V_t)$ must be convectively supersonic. This is a new finding, though intuitively expected from the condition established for the static jet.

2. *Collapse of Spectra from Unheated Jets at Angles* ≥ 130°

First, we consider the spectral characteristics for static jets in the peak radiation sector. Recently, Viswanathan [30] offered experimental evidence on the behavior of spectra from very low velocity unheated jets that showed:

1) The spectra at 90° and at lower angles have a universal shape; the spectral shape at large aft angles is completely different from the shape at 90°.

2) The spectra attain the large-scale similarity shape (with a sharper peak and rapid roll-off) for all jet velocities, at angles close to the jet axis.

3) There is a gradual change in spectral shape from a broad spectrum at the lower radiation angles to the large-scale similarity shape at angles close to the jet axis.

4) At ~160°, the jet spectra become independent of jet velocity and scale with Helmholtz number.

These trends have a bearing on the collapse of the spectra, as explained here. Analyses of the spectra indicate that in the intermediate angles, where there is a gradual transition in the spectral shape, an effective velocity would need to be defined. This velocity should be a simple function of the Strouhal number and the Helmholtz number, so as to cater to the spectral shapes outside the transitional angular range. The effective jet velocity is defined as

$$V_{\text{eff}} = V_j(1 - \alpha) + a\alpha$$

where α is a coefficient with a value from zero to unity. An effective Strouhal number is based on the effective velocity above. Note that $\alpha = 0$ yields the regular Strouhal number and $\alpha = 1$ yields the Helmholtz number. The spectra from unheated jets at several Mach numbers are collapsed with the effective Strouhal number in the

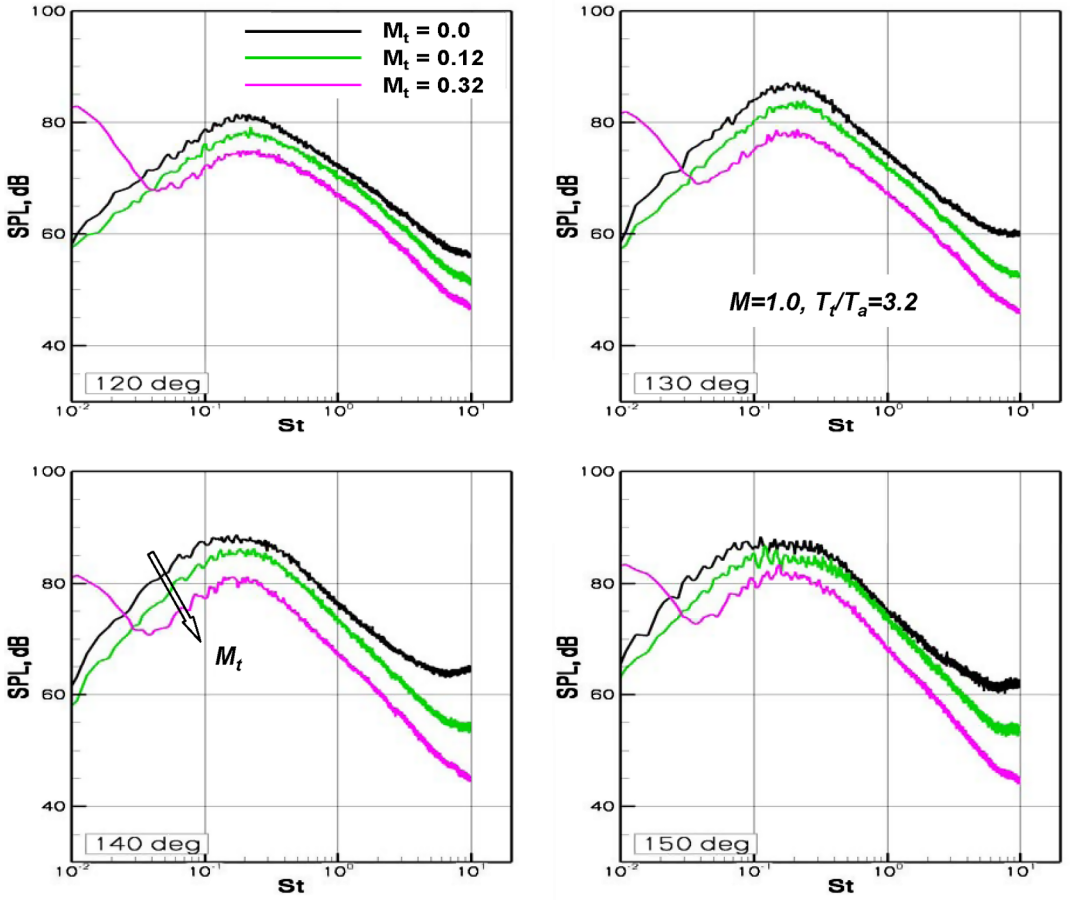

Fig. 19 Narrowband spectra at four aft angles. $M = 1.0$ and $T_t/T_a = 3.2$. and $M_t = 0.0$, 0.12 and 0.32.

angular range of 140 to 160° in 5° increments and displayed in Figs. 20–24. The corresponding values for α are 0.4, 0.7, 0.76, 0.8 and 1.0, respectively. As seen, very good collapse of the spectra is obtained with the selected values for α.

As shown in Sec. IV.B at the lower angles, an attempt is made to normalize the spectra with forward flight for an unheated $M = 1.0$ jet at various aft angles of 135, 140 and 150° in Fig. 25. Five tunnel Mach numbers of 0.0, 0.12, 0.16, 0.20 and 0.24 are considered. Interesting trends are observed:

1) At 135°, the spectral collapse for all tunnel Mach numbers is acceptable, except for the mismatch near the peak.

2) As we move aft to 140°, the data collapse gets worse. This is very obvious at the higher Strouhal numbers, with the spectral peak shifting to higher Strouhal numbers with increasing M_t. The arrow

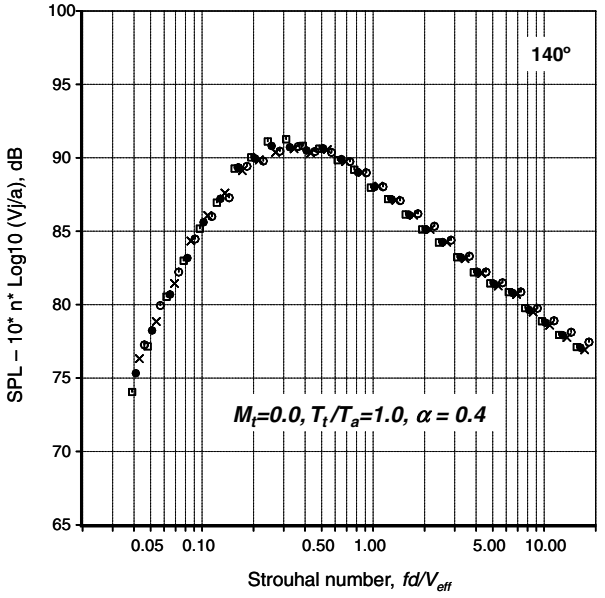

Fig. 20 Normalized spectra from static jets at 140°, $T_t/T_a = 1.0$. ○: $M = 0.6$; ×: $M = 0.7$; ●: $M = 0.8$; □: $M = 0.9$.

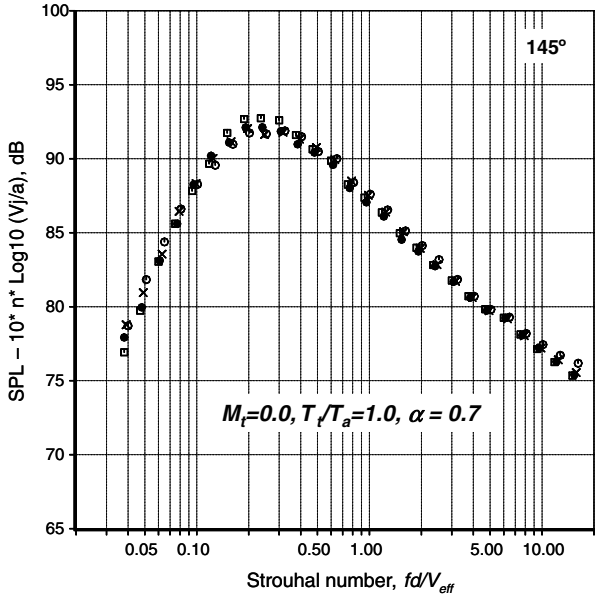

Fig. 21 Normalized spectra from static jets at 145°, $T_t/T_a = 1.0$. ○: $M = 0.6$; ×: $M = 0.7$; ●: $M = 0.8$; □: $M = 0.9$.

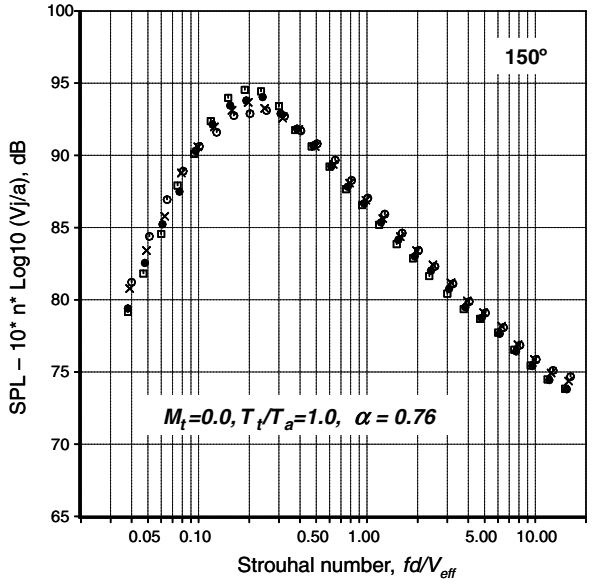

Fig. 22 Normalized spectra from static jets at 150°, $T_t/T_a = 1.0$. ○: $M = 0.6$; ×: $M = 0.7$; ●: $M = 0.8$; □: $M = 0.9$.

highlights this spectral shift, with the factor being ~1.6 when the tunnel Mach number is increased from 0.0 to 0.24.

3) This trend of shifting peak becomes very pronounced at 150°. At the higher frequencies, the spectra are spread out by a factor of ~3.0 when M_t is increased from 0.0 to 0.24. It is obvious that there is no collapse of the spectra; a closer examination at all angles reveals that the peak frequency and the entire spectra to the right of the spectral peak shift to higher frequencies (Strouhal numbers) with increasing M_t. The use of the modified Strouhal number would further exacerbate the observed trend, as the spectra obtained with forward flight will move to still higher Strouhal numbers because of the term $(V_j - V_t)$ in the denominator. Further, the use of the effective velocity will provide little benefit in collapsing the spectra because the jet velocity is held constant. Therefore, the scaling law that results in good collapse of the spectra at the lower polar angles is not valid in the peak radiation sector for unheated jets. The maximum angle at which the scaling law works seems to be ~125°, as shown in Fig. 12. There is a gradual degradation in the quality of the data collapse, as the radiation angle increases; this trend coincides with the angular range for the static case for which the value of α increases from 0.0 to 1.0. The reason for this behavior is unclear at the present time. The development of scaling laws for unheated jets for angles ≥ 130° requires special treatment and is deferred for the time being.

3. *Collapse of Spectra from Heated Jets at Angles* ≥ 130°

The spectral characteristics of heated jets under static conditions are considered. A similar exercise to that for the unheated jets was carried out for all the heated jets. A comprehensive analysis revealed that the regular Strouhal number with $\alpha = 0$ provides the best collapse for heated jets. Sample comparisons at 150° for two heated jets with $T_t/T_a = 1.8$ and 2.2 are depicted in Figs. 26 and 27, respectively. It appears that the use of the effective velocity is needed only for unheated jets; this is a peculiar phenomenon and has not been noted in any prior study. The reasons for the observed trends are unclear at the present time.

As before, the spectra with forward flight are normalized for the heated jets. The quantity $[\mathrm{SPL} + 10 * k * \mathrm{Log10}(V_j/(V_j - V_t))]$ is plotted on the y-axis against the regular Strouhal number. Sample results at various temperature ratios and radiation angles are now presented. Figure 28 depicts the normalized spectra at 140° for jets with $M = 1.0$ and $T_t/T_a = 2.2$ at five different tunnel Mach numbers of 0.0, 0.12, 0.16, 0.20 and 0.24. Figure 29a and 29b show the normalized spectra at 140° for jets with $M = 0.9$ and $T_t/T_a = 2.7$ at the several tunnel Mach numbers; the regular Strouhal number and the modified Strouhal number are used on the x-axis, respectively. Good collapse of the spectra is observed for these two cases in Figs. 28 and 29a with the regular Strouhal number. With the use of the modified Strouhal number, the spectra for the wind-on cases start moving to the right and the good collapse is destroyed.

Normalized spectra for a jet with a higher temperature ratio of 3.2 and a Mach number of 0.8, at still higher radiation angles of 145 and 150° are presented in Figs. 30 and 31, respectively. Two plots, with the regular Strouhal number and the modified Strouhal number are shown in Fig. 30. Once again, good agreements for the normalized spectra with the regular Strouhal number are seen at these aft angles, except at the highest three one-third octave bands, where a scatter of ±1.0 dB is observed. Attention is drawn to the fact that all the heated jets considered in this section are convectively subsonic. An examination of the normalized spectra in Figs. 28–31 indicates that the use of the modified Strouhal number based on $(V_j - V_t)$ would destroy the spectral collapse because the spectra obtained at different (V_t) would move to the right by differing amounts. Most of the past studies have used the modified Strouhal number as the nondimensional frequency; for example, the Society of Automotive Engineers prediction method, [31], incorporates the modified Strouhal number.

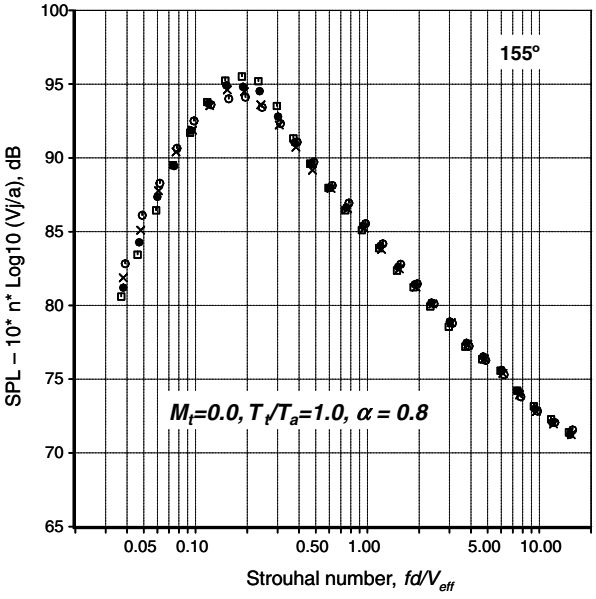

Fig. 23 Normalized spectra from static jets at 155°, $T_t/T_a = 1.0$. ○: $M = 0.6$; ×: $M = 0.7$; ●: $M = 0.8$; □: $M = 0.9$.

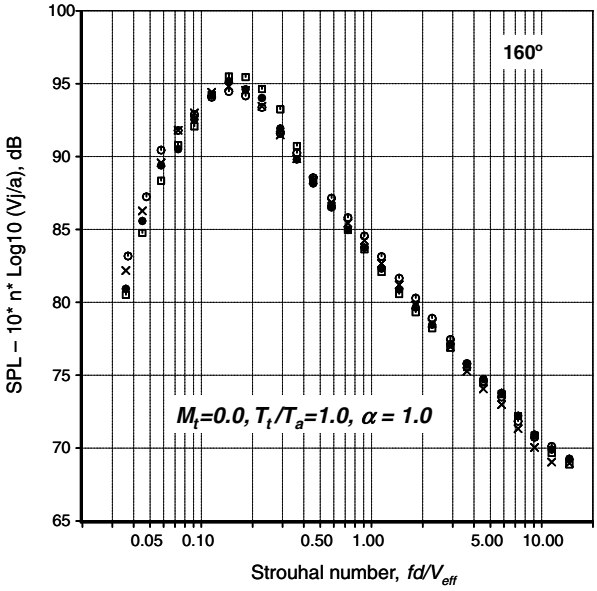

Fig. 24 Normalized spectra from static jets at 160°, $T_t/T_a = 1.0$. ○: $M = 0.6$; ×: $M = 0.7$; ●: $M = 0.8$; □: $M = 0.9$.

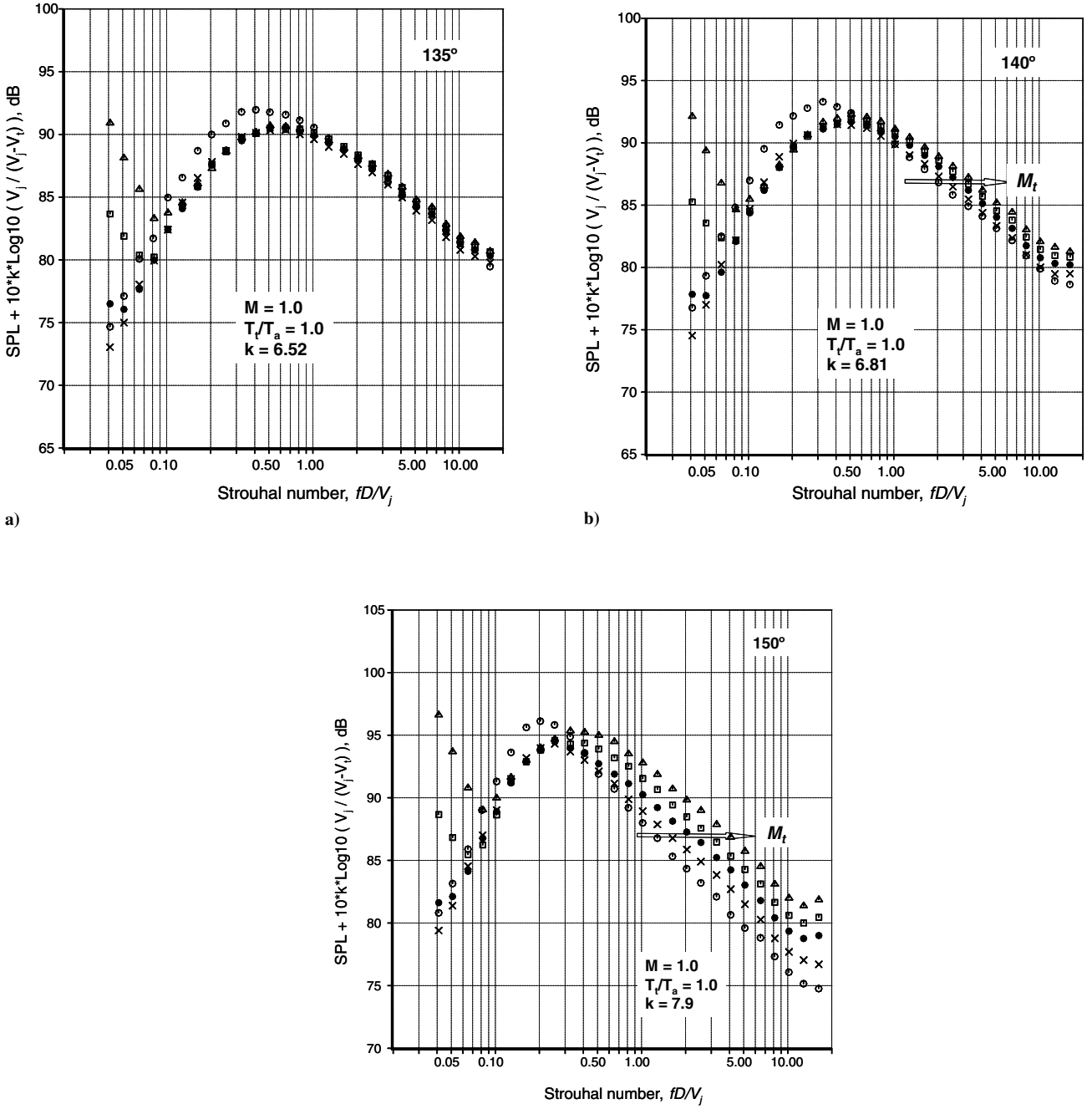

Fig. 25 Normalized one-third octave spectra at 150°. $M = 1.0$, $T_t/T_a = 1.0$. ○: $M_t = 0.0$; ×: $M_t = 0.12$; ●: $M_t = 0.16$; □: $M_t = 0.20$; △: $M_t = 0.24$.

It has been shown conclusively in Figs. 13, 14, and 28–31 that the regular Strouhal number is the correct nondimensional frequency for scaling spectra from jets with forward flight.

There is a stark contrast between unheated and heated jets, when the effects of forward flight are examined. The scaling law, in which the parameter $[\mathrm{SPL} + 10 * k * \mathrm{Log10}(V_j/(V_j - V_t))]$ is plotted against the regular Strouhal number, provides good collapse of the spectra from jets with and without forward flight at all angles from 50 to 150° for heated jets. For unheated jets, the angular range where the scaling law is obeyed is restricted to 50 to ∼125°. At larger aft angles, the scaling of spectra for both static jets and jets in the presence of a flight stream requires special consideration.

D. Effect of Forward Flight on Noise from Supersonic Jets

The effects of forward flight on shock-containing supersonic jets are now considered. Recall that a convergent nozzle has been used in this study. The flight effects on noise from convergent-divergent nozzles have been reported elsewhere; see [32]. The variations of the OASPL with radiation angle for a supersonic jet with $M = 1.37$ and $T_t/T_a = 2.7$, at six different tunnel Mach numbers of 0.0, 0.12, 0.16, 0.20, 0.24 and 0.28 are shown in Fig. 32. There is virtually no change in levels at the lower radiation angles of 50 to ∼90°; note that each division on the y-axis corresponds to 2 dB. The component of broadband shock-associated noise is dominant at the lower radiation angles; this angular range is highlighted in the figure. The turbulent mixing noise gradually becomes more prominent as we move aft and is the dominant component in the peak noise radiation sector. At the peak radiation angle of 135°, there is a reduction of ∼7 dB when the tunnel Mach number is increased from 0.0 to 0.28. Similar trends are observed for a jet with $M = 1.57$ and $T_t/T_a = 2.2$ in Fig. 33; five different tunnel Mach numbers of 0.0, 0.12, 0.16, 0.20 and 0.24 are considered. Again, there is relatively little change in levels at the lower angles and a ∼6 dB reduction at the peak radiation angle of

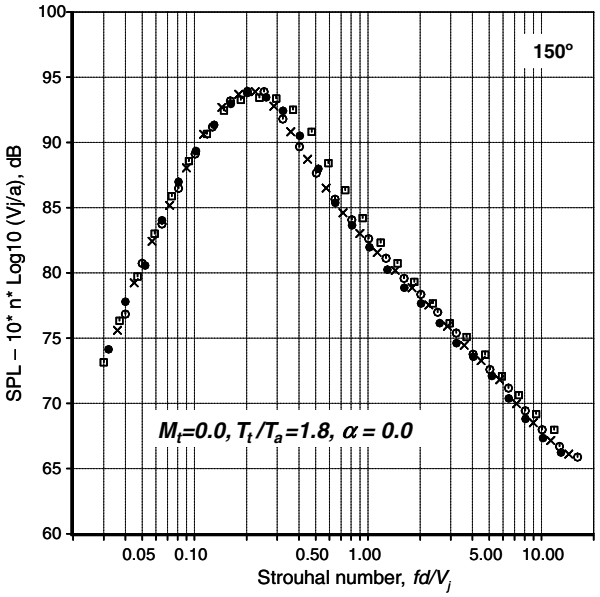

Fig. 26 Normalized spectra from static jets at 150°, $T_t/T_a = 1.8$. ○: $M = 0.6$; ×: $M = 0.7$; ●: $M = 0.8$; □: $M = 0.9$.

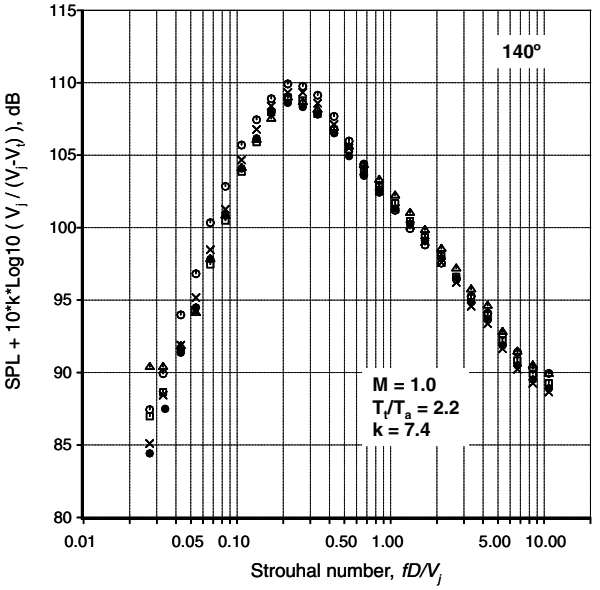

Fig. 28 Normalized one-third octave spectra at 140°. $M = 1.0$, $T_t/T_a = 2.2$. ○: $M_t = 0.0$; ×: $M_t = 0.12$; ●: $M_t = 0.16$; □: $M_t = 0.20$; △: $M_t = 0.24$.

135°. One can also appreciate the differences in the maximum noise levels for the two jet operating conditions in the two angular sectors, where the shock and mixing components are dominant. There is an increase of ∼5 dB at the lower angles due to the stronger shocks when the jet Mach number is increased from 1.37 to 1.57. There is only a minor change of ∼1 dB for the mixing noise component as the jet velocity varies only slightly, because the temperature ratio has been reduced from 2.7 to 2.2 for the higher Mach number jet.

The spectral characteristics for the $M = 1.57$ jet at two temperature ratios of 2.2 and 2.7 are now examined in Fig. 34. Four tunnel Mach numbers of 0.0, 0.16, 0.24 and 0.32 are considered. The power spectral densities (dB/Hz), at four radiation angles of 60, 80, 100 and 140°, span the angular range where the prominence of the shock component is progressively overtaken by the component of mixing noise. First of all, there is a reduction in the screech frequency when the flight Mach number is increased: examine the spectra at the lower angles for both jets. There is also a progressive reduction in the amplitude of the screech tone, with a complete elimination of the tone for the highest tunnel Mach number of 0.32. The changes to the broadband shock peak with flight Mach number is not pronounced; there seems to be a slight broadening of the spectral peak at 60° with increasing tunnel Mach number, but virtually no modifications at the higher angles. At 100°, the effect of forward flight on the turbulent mixing noise is evident at the lower frequencies, to the left of the screech tones. And finally, there is a reduction in levels with increasing M_t for the turbulent mixing noise component at 140°. Thus, there is a distinct difference in the effect of forward flight on the components of broadband shock noise and turbulent mixing noise.

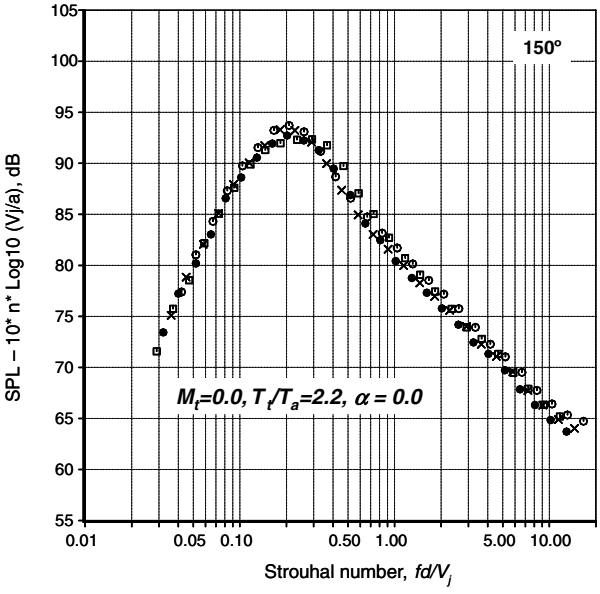

Fig. 27 Normalized spectra from static jets at 150°, $T_t/T_a = 2.2$. ○: $M = 0.6$; ×: $M = 0.7$; ●: $M = 0.8$; □: $M = 0.9$.

E. Prediction of Turbulent Mixing Noise from Jets in Forward Flight

An accurate method for the prediction of turbulent mixing noise is essential for a variety of practical applications. Such a methodology developed by Viswanathan [19,25] was shown to be superior to existing methods. A simple scaling formula for the spectra at every angle and temperature ratio is represented by the following equation:

$$\mathrm{SPL}\,(\theta, St) = F\left(\theta, St, \frac{T_t \text{ or } T_j}{T_a}\right)\left[\frac{V_j}{a}\right]^n, \qquad n = n\left(\theta, \frac{T_t \text{ or } T_j}{T_a}\right)$$

The SPL per unit area (or area-normalized SPL) at an arbitrary fixed distance is given by the product of a spectrum function and the velocity ratio raised to the velocity exponent n. The spectrum function F and exponent n, at a particular angle and temperature ratio, are obtained from experimental measurements. (T_j/T_a is the jet static temperature ratio). When the parameter $[\mathrm{SPL} - 10 * \mathrm{Log}_{10}(A/A_{\mathrm{ref}}) - 10 * n * \mathrm{Log}_{10}(V_j/a)]$ for one-third octave spectra or $[\mathrm{SPL} - 10 * \mathrm{Log}_{10}(A/A_{\mathrm{ref}}) - 10 * n * \mathrm{Log}_{10}(V_j/a) - 10 * \mathrm{Log}_{10}(D/V_j)]$ for narrowband spectra with constant bandwidth are plotted against the Strouhal number, a master spectral shape results for every angle and every temperature ratio. A is the nozzle exit area and A_{ref} is a reference area, which is taken to be one square inch here for convenience. This is the above spectrum function $F(\theta, St, T_{t,j}/T_a)$. The velocity exponent n has a unique value, and is calculated from the measured overall sound pressure levels at each angle, from jets of different (V_j/a), but fixed jet temperature ratio. A prediction involves just a reversal of the normalization process used to generate the master spectra.

The above methodology is restricted to static jets so far. Now, the scaling formula can be extended to jets in the presence of forward flight. The first step involves a static prediction. The results presented in this paper have established that the parameter $[\mathrm{SPL} + 10 * k * \mathrm{Log10}(V_j/(V_j - V_t))]$ collapses spectra from jets with forward flight. The second term provides a "flight effect" that must be applied

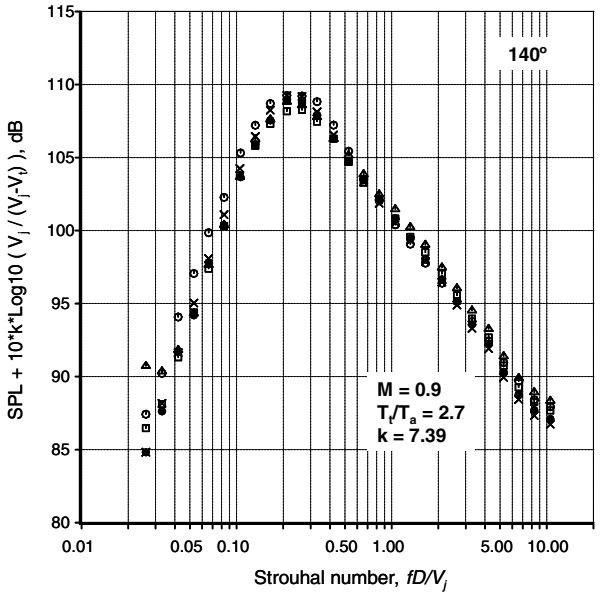

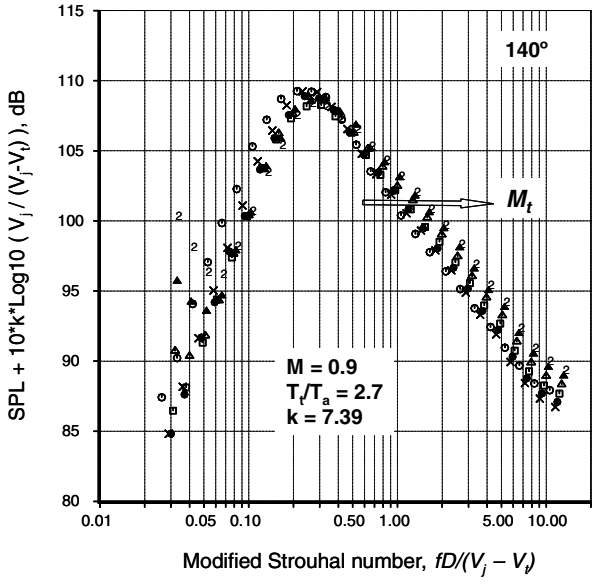

Fig. 29 Normalized one-third octave spectra at 140°. $M = 0.9$, $T_t/T_a = 2.7$. ○: $M_t = 0.0$; ×: $M_t = 0.12$; ●: $M_t = 0.16$; □: $M_t = 0.20$; △: $M_t = 0.24$; ▲: $M_t = 0.28$; 2: $M_t = 0.32$.

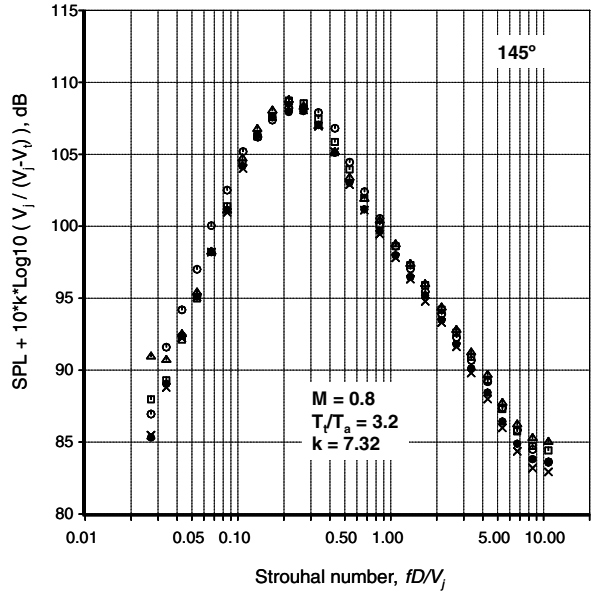

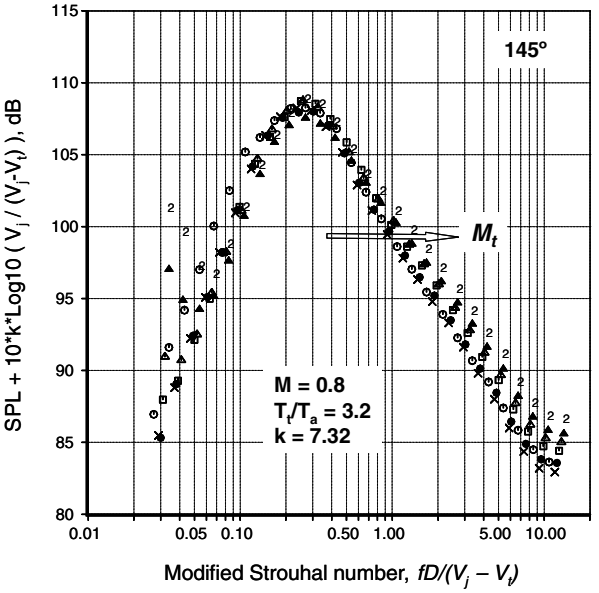

Fig. 30 Normalized one-third octave spectra at 145°. $M = 0.8$, $T_t/T_a = 3.2$. ○: $M_t = 0.0$; ×: $M_t = 0.12$; ●: $M_t = 0.16$; □: $M_t = 0.20$; △: $M_t = 0.24$; ▲: $M_t = 0.28$; 2: $M_t = 0.32$.

to the predicted static spectra, so as to obtain spectra in the presence of forward flight. This procedure can be written as

$$\mathrm{SPL}(\theta, St, V_t) = F\left(\theta, St, \frac{T_t \text{ or } T_j}{T_a}\right)\left[\frac{V_j}{a}\right]^n - 10 \times k \times \mathrm{Log10}\left[\frac{V_j}{(V_j - V_t)}\right] \qquad n = n\left(\theta, \frac{T_t \text{ or } T_j}{T_a}\right), \qquad k = k(\theta)$$

The values of the velocity exponent n, as a function of angle and temperature ratio, were presented in Viswanathan [19]; see Fig. 16 in that reference. The values of the flight velocity exponent (k) at each radiation angle have been determined from the current database and already presented in Fig. 8. Note that k does not have a dependence on the temperature ratio; no discernible trend could be established and the deviations from the mean line may be attributed to experimental scatter. An examination of Fig. 8 indicates that the scatter is within ± 0.5 of the mean line, with a tighter collapse at the lower radiation angles. Though it is possible to use the tabulated values of k directly, a mean value at each angle would simplify the prediction procedure. One could estimate the magnitude of the error due to the use of an average value for k, as shown in Table 1. The variations of the introduced error (ΔdB) with V_t for three different values of V_j are presented in Table 1. The magnitude of the error increases with V_t as expected and has the highest value for low V_j. For heated jets, with $V_j \approx 1600$ ft/s, the error is ≤ 0.5 dB, even for a flight speed of 350 ft/s. Therefore, the relation $k = k(\theta)$ does not introduce any significant error. For the sake of perspective, it is noted that the accuracy of the spectral measurements under static conditions is within ± 0.5 dB (or smaller), as amply demonstrated in [17–22]. It should be appreciated then that the error due to the assumption of $k = k(\theta)$ is of the same magnitude as the experimental uncertainty.

It is quite amazing that the characteristics of the mixing noise spectra at all angles, with or without the presence of forward flight, can be represented by a single equation. This fact is all the more remarkable as no questionable assumptions have been invoked in the development of the above equation. A complete method for the prediction of turbulent mixing noise with flight effects is now available. A notable feature of the prediction method is highlighted:

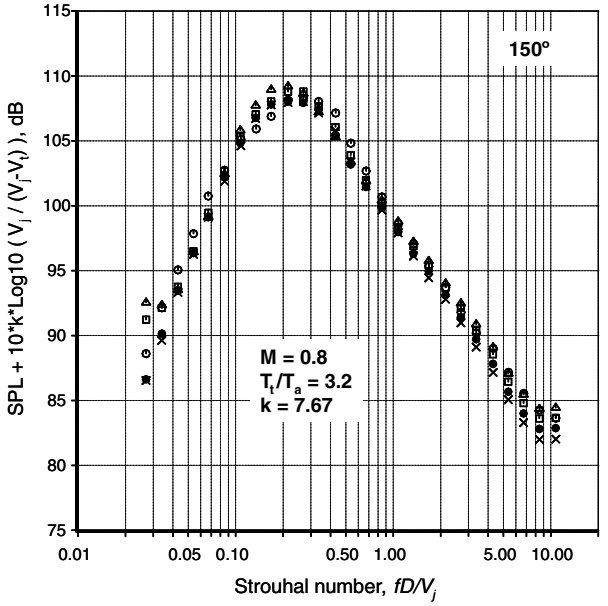

Fig. 31 Normalized one-third octave spectra at 150°. $M = 0.8$, $T_t/T_a = 3.2$. ○: $M_t = 0.0$; ×: $M_t = 0.12$; ●: $M_t = 0.16$; □: $M_t = 0.20$; △: $M_t = 0.24$.

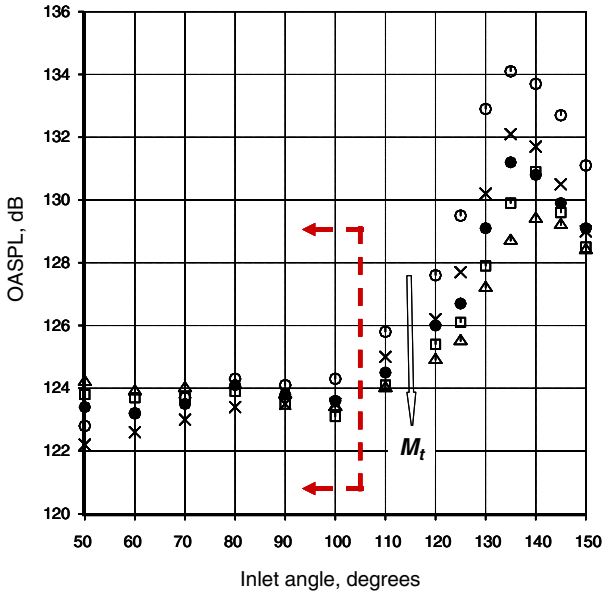

Fig. 33 Directivity of OASPL for $M = 1.57$ and $T_t/T_a = 2.2$ jet. ○: $M_t = 0.0$; ×: $M_t = 0.12$; ●: $M_t = 0.16$; □: $M_t = 0.20$; △: $M_t = 0.24$.

because the prediction originates with a static spectrum, uncontaminated by tunnel noise floor (especially at the lower frequencies), the predicted flight spectrum is devoid of the turn-up at the lower frequencies due to tunnel noise. That is, the proper spectral shape is maintained over the entire frequency range for the spectrum with forward flight.

A few outstanding issues remain. The scaling and prediction of spectra from unheated jets for angles $\geq 130°$ would require some additional analyses. The quantification of the effects associated with nonlinear propagation at higher jet velocities, for supersonically convective jets, entails the solution of the Burgers equation, with the initial condition provided by the measured pressure-time signal at a certain distance close enough to be in the far field. In general, the increase in spectral levels at the higher frequencies is a function of 1) the propagation distance (number of wavelengths), 2) the relative jet velocity ($V_j - V_t$), 3) the radiation angle, and 4) the frequency. However, the need for solving the Burgers equation is not practical and does not fall under the ambit of a simple prediction method. Recent theoretical and computational efforts at Pennsylvania State University (see for example [33,34]) offer a way forward. Perhaps a look-up table that provides a dB correction as a function of the four controlling parameters listed above would permit the prediction of the turbulent mixing noise at supersonically convective velocities. Such an approach is currently being investigated.

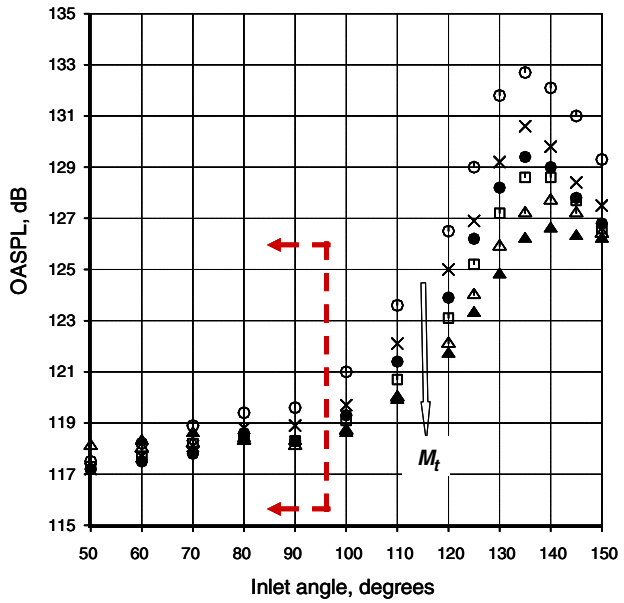

Fig. 32 Directivity of OASPL for $M = 1.37$ and $T_t/T_a = 2.7$ jet. ○: $M_t = 0.0$; ×: $M_t = 0.12$; ●: $M_t = 0.16$; □: $M_t = 0.20$; △: $M_t = 0.24$, ▲: $M_t = 0.28$.

It is apropos at this juncture to contrast the results of the current study from those of past studies. It was noted in Sec. IV.B that a flight velocity exponent of ~5.5 at 90° was calculated from the Lockheed measurements, whereas it is ~3.0 in the current data. A closer examination of Figure 1.1 in [11] reveals that the values at 90° range from ~3.2 to ~5.5 for model-scale tests. The values obtained from flight tests are significantly different. However, a value of ~5 to ~5.5 for the flight exponent has been generally assumed at 90°. Let us re-examine Fig. 8 in the current paper. There is tight collapse of k in the angular range of 50 to 90°, and the values vary from ~2.9 to ~3.5. It is impressive that the scatter is minor for eight different jet conditions (Mach numbers and temperature ratios). Such a trend has not been demonstrated in any past study. In addition, it has been demonstrated convincingly that:

1) The use of the computed k here leads to excellent collapse of the spectra at all the angles.

2) The calculated values for the flight exponents are accurate and are applicable over a wider range of higher tunnel Mach numbers, even if they are obtained only from the data at lower M_t. Figures 11 and 12 bear out this observation.

As a further check, the following exercise is carried out. The spectra for the $M = 1.0$ and $T_t/T_a = 1.0$ are normalized with a flight exponent value of 5.5 and the resulting normalized spectra are shown in Fig. 35. There is no collapse of the spectra! Contrast this trend with that observed in Fig. 9a for the same test condition, but normalized with the computed value for k of 3.44. It is obvious that an exponent of 5.5 completely destroys the excellent spectral collapse obtained with an exponent of 3.44. Given the demonstrated goodness of the spectral collapse at all angles, the values for k depicted in Fig. 8 are deemed to be accurate. Viswanathan [17–19,22,35] has reported extensively on issues associated with data quality; it has been shown that most of the past measurements suffer from serious problems, even under static conditions. Measurements in the presence of a flight stream are subject to additional problems, as discussed in the Introduction section. Perhaps it should not come as a surprise that there is considerable scatter in the value of k and doubts about the accuracy of the flight exponents obtained from the older measurements.

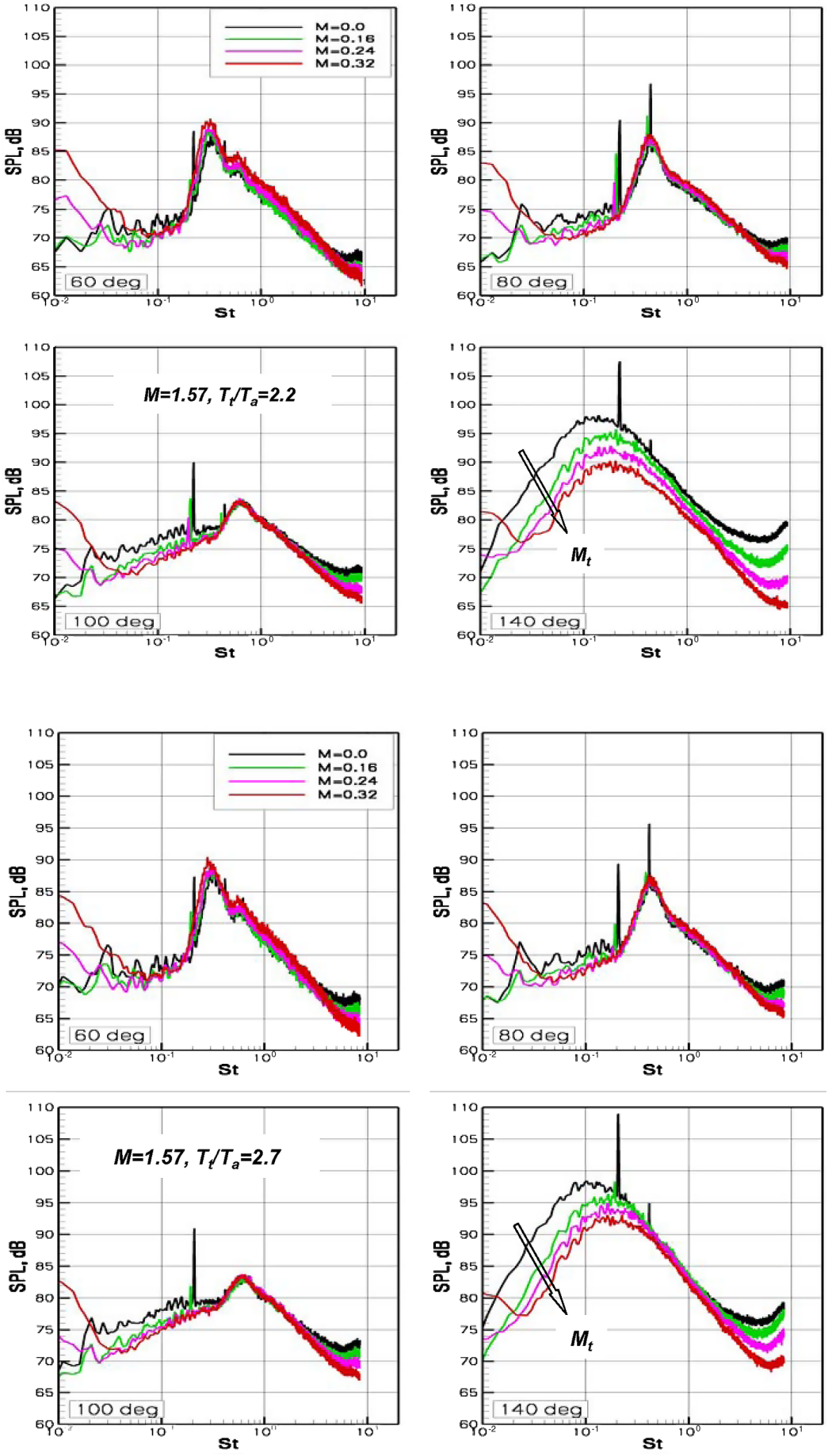

Fig. 34 Effect of forward flight on narrowband spectra, $M = 1.57$. top: $T_t/T_a = 2.2$; bottom: $T_t/T_a = 2.7$.

Table 1 Error in dB due to scatter in k

V_t, ft/s	$V_j = 1000$, ft/s ΔdB	$V_j = 1600$, ft/s ΔdB	$V_j = 2200$, ft/s ΔdB
0	0	0	0
100	0.23	0.14	0.10
150	0.35	0.21	0.15
200	0.48	0.29	0.21
250	0.62	0.37	0.26
300	0.77	0.45	0.32
350	0.94	0.54	0.38

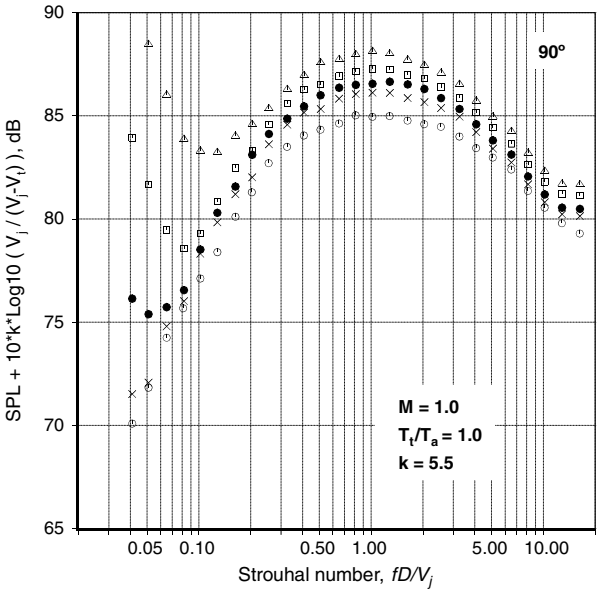

Fig. 35 Normalized one-third octave spectra at 90°. $M = 1.0$, $T_t/T_a = 1.0$. ○: $M_t = 0.0$; ×: $M_t = 0.12$; ●: $M_t = 0.16$; □: $M_t = 0.20$; △: $M_t = 0.24$.

V. Conclusions

The effects of forward flight on single-stream jet noise are investigated in this study. Both turbulent mixing noise and broadband shock-associated noise are considered. Far-field spectral measurements have been made over a wide range of jet operating conditions and at seven tunnel Mach numbers, in an open freejet anechoic facility. The tunnel Mach numbers (M_t) spans a range from 0.0 to 0.32. The as-measured data are corrected for the effects due to convection by the tunnel flow and the refraction of the acoustic rays through the tunnel shear layer, using the procedure developed by Amiet [9,12]. An interpolation of the resulting spectra at the true radiation angles to the radiation angles for the static case (fixed microphone angles) allows the direct comparison of the spectra obtained at various tunnel Mach numbers. The effects of flight on spectra at various angles need to be modeled for the development of a practical prediction scheme for jet noise. The recent scaling method of Viswanathan [19,25] provides very good collapse of the spectra at all angles and over the entire frequency range without any theoretical assumptions, thereby permitting the development of an accurate prediction method for jets in a static environment. One of the goals of the present study is the extension of the basic methodology to include flight effects.

The values of the flight velocity exponent k have been calculated at all angles from the database. The flight velocity exponent has no discernible dependence on jet Mach number or temperature ratio. There is a well defined variation with angle: a slow increase from ∼2.9 to ∼3.5 at the lower polar angles from 50 to ∼105° and a steeper increase from ∼3.5 to ∼7.6 from ∼105 to 150°. Two different characteristic velocities may be identified for jets in forward flight: jet velocity V_j and relative velocity $(V_j - V_t)$. The suitability of both for collapsing spectra from jets with forward flight has been examined. When the parameter $[\mathrm{SPL} + 10 * k * \mathrm{Log10}(V_j/(V_j - V_t))]$ is plotted against the regular Strouhal number (fD/V_j), the spectra collapse on to a single curve over the entire Strouhal number range. Though the Strouhal numbers based on both provide good collapse of the spectra at the lower polar angles, the jet velocity rather than $(V_j - V_t)$ is shown to be the correct characteristic velocity at large aft angles. Thus, it is established that the regular Strouhal number based on V_j is the correct nondimensional frequency for scaling spectra. The negligible dependence of the flight velocity exponent on jet conditions allows for the following practical benefit: it is possible to predict the flight effect for lower velocity jets for which the measurement of flight effect may not be feasible because of high-tunnel-noise floor. This key finding perhaps represents the greatest value of this investigation.

The scaling of spectra at large aft angles is not straightforward and additional issues need to be considered. The first one pertains to the effects due to nonlinear propagation. Viswanathan [21,27] offered experimental evidence that this phenomenon is observed when the convective velocity becomes supersonic. For jets in the presence of forward flight, it is established that the phenomenon of nonlinear propagation is observed when the relative velocity $(V_j - V_t)$ exceeds this threshold value. This is a new result and has not been reported in any prior study. This phenomenon has a profound bearing in collapsing spectra from jets which are supersonically convective; a separate computational method or a simplified procedure is required to account for the transfer of energy to the higher frequencies and the resultant increase in the spectral levels at these frequencies.

An effective jet velocity, which is a combination of both the jet velocity and the ambient speed of sound, is required to collapse spectra from unheated jets at large aft angles. An effective Strouhal number, which shifts gradually from the regular Strouhal number at angles $\leq \sim 130°$ to the Helmholtz number at 160°, is shown to collapse the static spectra from unheated jets at all angles. In the presence of forward flight, however, the spectral collapse becomes progressively worse as the radiation angle increases from ∼135°. The spectral peak shifts monotonically to higher Strouhal numbers with increasing V_t and the spectra at the higher frequencies to the right of the spectral peak spread apart. The degree of the mismatch becomes more pronounced with increasing radiation angle. Good spectral collapse, without the introduction of ad-hoc functions, is not possible for angles $\geq \sim 130°$ for unheated jets.

The use of an effective velocity is not required for heated jets; the regular Strouhal number is the correct nondimensional frequency at all angles, with or without forward flight. Good spectral collapse is obtained at all angles when the parameter $[\mathrm{SPL} + 10 * k * \mathrm{Log10}(V_j/(V_j - V_t))]$ is plotted against the regular Strouhal number (fD/V_j). There is a stark contrast between unheated and heated jets, in the scaling of spectra at large aft angles. This characteristic difference is true whether there is forward flight or not.

The effect of forward flight on broadband shock-associated noise is much different from that on turbulent mixing noise. There is virtually no effect on the OASPL at the lower angles, where shock noise is dominant. There is a reduction in the screech frequency when the flight Mach number is increased. There is also a progressive reduction in the amplitude of the screech tone, with a complete elimination of the tone for higher forward flight speeds. Spectrally, the changes to the broadband shock noise with flight Mach number are minor.

The goal of extending the prediction method based on the scaling laws for static jets has been accomplished. An additional term that provides a flight effect can be applied to the predicted static spectra, so as to obtain spectra in the presence of forward flight. The spectral characteristics of jets in forward flight can be represented simply by

$$\mathrm{SPL}(\theta, St, V_t) = F\left(\theta, St, \frac{T_t \text{ or } T_j}{T_a}\right)\left[\frac{V_j}{a}\right]^n - 10 \times k \times \mathrm{Log10}\left[\frac{V_j}{(V_j - V_t)}\right] \qquad n = n\left(\theta, \frac{T_t \text{ or } T_j}{T_a}\right), \qquad k = k(\theta)$$

It is quite remarkable that the characteristics of the mixing noise spectra from single-stream jets at all angles, with or without the presence of forward flight, can be represented by a single equation. This fact is all the more noteworthy as no questionable assumptions have been invoked in the development of the above equation. A notable feature of the prediction method is highlighted: because the prediction originates with a static spectrum, uncontaminated by tunnel noise floor (especially at the lower frequencies), the predicted flight spectrum is devoid of the turn-up at the lower frequencies due to tunnel noise. That is, the proper spectral shape is maintained over the entire frequency range for the spectrum with forward flight. A complete method for the prediction of turbulent mixing noise with flight effects is now available for convectively subsonic jets.

References

[1] Crighton, D. G., Ffowcs Williams, J. E., and Cheeseman, I. C., "The Outlook for Simulation of Forward Flight Effects on Aircraft Noise," AIAA Paper 76-530, 1976.

[2] Von Glahn, U., Groesbeck, D., and Goodykoontz, J., "Velocity Decay and Acoustic Characteristics of Various Nozzle Geometries in Forward Flight," AIAA Paper 73-629, 1973.

[3] Cocking, B. J., and Bryce, W. D., "Subsonic Jet Noise in Flight Based on Some Recent Wind Tunnel Results," AIAA Paper 75-462, 1974.

[4] Bushell, K. W., "Measurement and Prediction of Jet Noise in Flight," AIAA Paper 75-461, 1975.

[5] Packman, A. B., Ng, K. W., and Paterson, R. W., "Effect of Simulated Forward Flight on Subsonic Jet Exhaust Noise," AIAA Paper 75-869, 1975.

[6] Plumblee, H. E., "Effects of Forward Velocity on Turbulent Jet Mixing Noise," NASA CR-2702, 1976.

[7] Tanna, H. K., and Morris, P. J., "In-Flight Simulation Experiments on Turbulent Jet Mixing Noise," *Journal of Sound and Vibration*, Vol. 53, No. 3, 1977, pp. 389–405. doi:10.1016/0022-460X(77)90422-9

[8] Cocking, B. J., "A Prediction Method for the Effects of Flight on Subsonic Jet Noise," *Journal of Sound and Vibration*, Vol. 53, No. 3, 1977, pp. 435–453. doi:10.1016/0022-460X(77)90425-4

[9] Amiet, R. K., "Correction of Open Jet Wind Tunnel Measurements for Shear Layer Refraction," AIAA Paper 75-532, 1975.

[10] Morfey, C. L., and Tester, B. J., "Noise Measurements in a Free Jet Flight Simulation Facility: Shear Layer Refraction and Facility-to-Flight Corrections," *Journal of Sound and Vibration*, Vol. 54, No. 1, 1977, pp. 83–106. doi:10.1016/0022-460X(77)90408-4

[11] Ahuja, K. K., Tester, B. J., and Tanna, H. K., "The Free Jet as a Simulator of Forward Velocity Effects on Jet Noise," NASA CR-3056, Oct. 1978.

[12] Amiet, R. K., "Refraction of Sound by a Shear Layer," *Journal of Sound and Vibration*, Vol. 58, No. 4, 1978, pp. 467–482. doi:10.1016/0022-460X(78)90353-X

[13] Hoch, R. G., and Berthelot, M., "Use of the Bertin Aérotrain for the Investigation of Flight Effects on Aircraft Engine Exhaust Noise," *Journal of Sound and Vibration*, Vol. 54, No. 2, 1977, pp. 153–172. doi:10.1016/0022-460X(77)90021-9

[14] Drevet, P., Duponchel, J. P., and Jacques, J. R., "The Effect of Flight on Jet Noise as Observed on the Bertin Aérotrain," *Journal of Sound and Vibration*, Vol. 54, No. 2, 1977, pp. 173–201. doi:10.1016/0022-460X(77)90022-0

[15] Norum, T. D., and Shearin, G., "Shock Structure and Noise of Supersonic Jets in Simulated Flight to Mach 0.4," NASA TP-2785, 1988.

[16] Norum, T. D., and Brown, M. C., "Simulated High Speed Flight Effects on Supersonic Jet Noise," AIAA Paper 93-4388, 1993.

[17] Viswanathan, K., "Jet Aeroacoustic Testing: Issues and Implications," *AIAA Journal*, Vol. 41, No. 9, 2003, pp. 1674–1689. doi:10.2514/2.7313

[18] Viswanathan, K., "Aeroacoustics of Hot Jets," *Journal of Fluid Mechanics*, Vol. 516, Oct. 2004, pp. 39–82. doi:10.1017/S0022112004000151

[19] Viswanathan, K., "Scaling Laws and a Method for Identifying Components of Jet Noise," *AIAA Journal*, Vol. 44, No. 10, Oct. 2006, pp. 2274–2285. doi:10.2514/1.18486

[20] Shields, F. D., and Bass, H. E., "Atmospheric Absorption of High Frequency Noise and Application to Fractional-Octave Band," NASA CR 2760, 1977.

[21] Viswanathan, K., "Does a Model Scale Nozzle Emit the Same Jet Noise as a Jet Engine?," *AIAA Journal*, Vol. 46, No. 2, 2008, pp. 336–355. doi:10.2514/1.18019

[22] Viswanathan, K., "Instrumentation Considerations for Accurate Jet Noise Measurements," *AIAA Journal*, Vol. 44, No. 6, 2006, pp. 1137–1149. doi:10.2514/1.13518

[23] Viswanathan, K., "Distributions of Noise Sources in Heated and Cold Jets: Are They Different?," *International Journal of Aeroacoustics*, Vol. 9, Nos. 4–5, 2010, pp. 589–626. doi:10.1260/1475-472X.9.4-5.589 (invited article).

[24] Michalke, A., and Michel, U., "Prediction of Jet Noise in Flight from Static Tests," *Journal of Sound and Vibration*, Vol. 67, No. 3, 1979, pp. 341–367. doi:10.1016/0022-460X(79)90541-8

[25] Viswanathan, K., "Improved Method for Prediction of Noise from Single Jets," *AIAA Journal*, Vol. 45, No. 1, Jan. 2007, pp. 151–161. doi:10.2514/1.23202

[26] Viswanathan, K., "Mechanisms of Jet Noise Generation: Classical Theories and Recent Developments," *International Journal of Aeroacoustics*, Vol. 8, No. 4, 2009, pp. 355–408. doi:10.1260/147547209787548949

[27] Viswanathan, K., "Recent Advances in Jet Noise Suppression," International Symposium on Recent Advances in Aeroacoustics and Active Flow-Combustion Control, in Honor of Professor Ffowcs-Williams, Goa, India, Jan. 2005.

[28] Morfey, C. L., and Howell, G. P., "Nonlinear Propagation of Aircraft Noise in the Atmosphere," *AIAA Journal*, Vol. 19, No. 8, 1981, pp. 986–992. doi:10.2514/3.51026

[29] Benoit, P. P., Viswanathan, K., and McLaughlin, D. K., "Acoustic Pressure Forms Measured in High Speed Jet Noise Experiencing Nonlinear Propagation," *International Journal of Aeroacoustics*, Vol. 5, No. 2, 2006, pp. 193–215. doi:10.1260/147547206777629835

[30] Viswanathan, K., "Investigation of Noise Source Mechanisms in Subsonic Jets," *AIAA Journal*, Vol. 46, No. 8, 2008, pp. 2020–2032. doi:10.2514/1.34471

[31] "Gas Turbine Exhaust Noise Prediction," Society of Automotive Engineers ARP876, Rev. D, 1994.

[32] Viswanathan, K., Krothapalli, A., Seiner, J. M., Czech, M. J., Greska, B., and Jansen, B. J., "Assessment of Noise Reduction Concepts for Fighter Aircraft Application in Simulated Forward Flight," AIAA Paper 2010-14, Jan. 2010 (submitted for publication to *Journal of Aircraft*).

[33] Saxena, S., Morris, P. J., and Viswanathan, K., "Algorithm for the Nonlinear Propagation of Broadband Jet Noise," *AIAA Journal*, Vol. 47, No. 1, 2009, pp. 186–194. doi:10.2514/1.38122

[34] Lee, S., Morris, P. J., and Brentner, K. S., "Nonlinear Acoustic Propagation Predictions with Applications to Aircraft and Helicopter Noise," AIAA Paper 2010-1384, Jan. 2010.

[35] Viswanathan, K., "Best Practices for Accurate Measurement of Pure Jet Noise," *International Journal of Aeroacoustics*, Vol. 9, Nos. 1–2, 2010, pp. 145–206 (invited article). doi:10.1260/1475-472X.9.1-2.145

A. Lyrintzis
Associate Editor